Genome-wide identification and expression analysis of the GRAS transcription factor family and its expression profiles in Elymus sibiricus

Xiang Meng
Xinjiang Agricultural University
Fang Liu
National Animal Husbandry Service
Lin Ma
Chinese Academy of Agricultural Sciences
Wenhui Liu
Oinghai University
Jun Tang
Chinese Academy of Agricultural Sciences
Kaiqiang Liu
Oinghai University
Tong Miao
Chinese Academy of Agricultural Sciences
Dengxia Yi
Chinese Academy of Agricultural Sciences
Jun Hong
National Animal Husbandry Service
Xiaoran Ma
Chinese Academy of Agricultural Sciences
Miaomiao Huang
Oinghai University
Zeliang Ju
Oinghai University
Xuemin Wang
wangxuemin@caas.cn
Chinese Academy of Agricultural Sciences
Kaiyun Xie
Xinjiang Agricultural University

Research Article

Keywords: E. sibiricus, GRAS gene family, evolutionary relationships, gene expression, abiotic stress

Posted Date: October 8th, 2025

DOI: https://doi.org/10.21203/rs.3.rs-7355432/v1

Additional Declarations: No competing interests reported.

Version of Record: A version of this preprint was published at BMC Genomics on January 10th, 2026. See the published version at https://doi.org/10.1186/s12864-025-12349-4.

Abstract

Background: *Elymus sibiricus* is widely utilized for establishing of high-yield artificial grasslands due to its remarkable productivity and strong resistance to environmental stresses, making it an excellent forage species. *GRAS* transcription factors play a pivotal role in regulating plant growth, development, and responses to abiotic stress. Although the *GRAS* gene family has been identified in various plant species, its identification and function in *E. sibiricus* remain largely unexplored.

Result: A comprehensive genome-wide analysis Identified a total of 130 *EsGRAS* genes in *E. sibiricus*. Comprehensive analyses, including chromosomal distribution, gene structure, conserved motifs, cis-acting regulatory elements and evolutionary relationships, were conducted. Protein-protein interaction network analysis predicted that GID1, GA2OX, GA3OX, PAT1, PHYA, and NSP2 may serve as central nodes in *GRAS*-mediated regulatory pathways. Expression profiling revealed that most *EsGRAS* geneswere highly expressed in seedling tissues. Additionally, multiple *EsGRAS* genes showed differential expression in response to salt, drought, ABA, and GA treatments, indicating their potential involvement in abiotic stress tolerance.

Conclusion: The study systematically characterized the GRAS gene family in *E. sibiricus*. Identifying 130 members and revealing their diverse structural features and expression patterns. Notably, *EsGRAS128*, *EsGRAS90*, *EsGRAS95*, and *EsGRAS113*genes exhibited both constitutive expression and strong responsiveness under multiple abiotic stresses, suggesting their potential regulatory roles. These findings provide a foundation for understanding the genetic evolution and biological functions of the *GRAS*gene family in *E. sibiricus*, for further functional studies and may facilitate molecular breeding strategies to enhance stress resilience in *E. sibiricus* and related forage species.

1. Introduction

GRAS genes constitute a plant-specific transcription factor family that plays essential roles in regulating plant growth, development, signaling pathways, and responses to environmental stimuli [1]. The acronym *GRAS* is derived from the first identified members: *GAI* (Gibberellic Acid Insensitivity), *RGA* (Repressor of GA1-3 mutant), and *SCR* (Scarecrow), whose encoded proteins are involved in diverse physiological processed across plant species [2]. GRAS proteins typically consist of 400–770 amino acids and are characterized by a highly conserved C-terminal region containing five typical motifs: LHRI, VHIID, LHRII, PFYRE, and SAW. Among them, the VHIID domain is crucial for mediating protein-protein interactions, while the variable N-terminal region contributes to functional diversification within the family [3]. Phylogenetic analysis in *Arabidopsis thaliana* categorized GRAS proteins into eight subfamilies—DELLA, SCR, and HAM-with subsequent studies identifying additional groups such as DLT and SCL4/7 [4]. Functionally, *GRAS* transcription factors are involved in multiple developmental pathways, including gibberellin signal, root architecture formation, meristem development, and leaf patterning [5–8]. Of particular importance, members of the DELLA subfamily act as serve central repressors in the gibberellin signaling pathway, modulating plant growth in response to hormonal cues [9].

In *A. thaliana*, DELLA proteins—including GAI, RGA, and RGL1-3—function as key negative regulators of gibberellin (GA) signaling. These proteins interact with the GA receptor GID1 to form complexes that are subsequently degraded by the 26S proteasome. This degradation alleviates the repressive effects of DELLA proteins on GA-responsive genes, thereby facilitating plant growth and development [10]. Members of the PAT1 subfamily are involved in phytochrome A-mediated light signaling and contribute to growth regulation under variable light conditions. In *Vitis vinifera*, PAT1-type GRAS proteins also participate in cold stress responses by modulating jasmonic acid biosynthesis [11]. The SCR (Scarecrow) and SHR (Short Root) subfamilies are crucial for root radial patterning. SCR is predominantly expressed in endodermis/cortex initial cells, where it maintains stem cell homeostasis in the root apical meristem by suppressing cytokinin signaling and promoting mitotic activity [12]. Conversely, the SHR protein facilitates asymmetric cell division to establish ground tissues (endodermis and cortex) and promotes endodermis specification by regulating gene expression in asjacent cell layers. Additionally, SCL3 modulates cellular differentiation and elongation in root developmental zones [13]. Several orthologous genes—*Ls* (Lateral Suppressor) in tomato (*Solanum lycopersicum*), *LAS* (Lateral Suppressor) in *A. thaliana*, and *MOC1* (Monoculm 1) in rice (*Oryza sativa*)—collectively regulate axillary bud initiation and outgrowth [14]. In rice, *OsSLR1*, a DELLA subfamily member - regulates culm elongation and tiller number by suppressing GA signaling. The *osslr1* mutants displays slender culms and enhanced disease resistance. *OsSLR1* also interacts with *OsUDT1* to regulate tapetum-specific gene expression, which is critical for pollen wall development. In *Liriodendron chinense*, *LcGRAS* modulates plant development by regulating the expression of cell proliferation-related genes such as *OsmiR396a*/*OsGRFs* [15]. In rice, DELLA proteins govern growth and development via the GA signaling pathway [16]. Overall, DELLA proteins serve as key modulators of phytohormone signaling, contributing to the regulation of plant architecture, including height, leaf morphogenesis, and reproductive development.

GRAS gene family coordinates plant growth, development, and stress resilience by integrating phytohormone signaling pathways, tissue morphogenesis, and adaptive responses to environmental stimuli [17]. Under salt stress conditions, the *GRAS* transcription factors modulate key hormonal pathways, particularly those involving gibberellin (GA) and abscisic acid (ABA), to enhance stress resilience. For instance, in *Populus euphratica*, *PeSCL7* expression is induced by salt treatment, and its overexpression improves salt tolerance in transgenic *A. thaliana* plants [18]. In *Ricinus communis* (castor bean), salt stress upregulates *RcGRAS14*, *RcGRAS21*, and *RcGRAS35*, while suppressing *RcGRAS1* and *RcGRAS10*expression [19]. These findings suggest that *GRAS* genes may confer salt tolerance by modulating root growth and development and, thereby enhancing water and nutrient acquisition. In *A. thaliana*, the *SCL3* subfamily integrates multiple signaling cues during root cell elongation to ensure the proper functioning of the GA pathway and modulate cellular expansion [20]. Overexpression of *SlGRAS40* leads toelevated accumulation of proline and soluble sugars under drought stress, contributing to osmotic homeostasismaintaining and improved stress tolerance in *Solanum lycopersicum* [21]. Similarly, in *Liriodendron chinense*, members of the *LcPAT* subfamily (e.g., PAT3, PAT4, PAT5) are significantly upregulated after 24 hours of drought treatment, potentially functioning through the induction of cold-regulated (COR) proteins [22].

GRAS genes also interact with broader transcriptional networks to confer drought resistance. For example, in Potato (*Solanum tuberosum*), *StNAC053* enhances drought resistance by upregulating *DREB* (Dehydration-Responsive Element Binding) and *NAC* (NAM/ATAF/CUC) transcription factors [23]. In *A. thaliana*, and major cereal crops, DELLA proteins including GAI, RGA, RGL2, SLR1, and Rht-B1/Rht-D1 serve as central repressors within the GA signaling pathway, balancing growth with stress defense [24]. Concurrently, the SCR subfamily member *OsGRAS32* in rice has been identified as a key regulator of GA metabolism and plays aa role in developmental processes under stress conditions [25]. The *GRAS* gene family is also implicated in ABA signaling, potentially modulates key components such as PYR/PYL/RCAR receptors, PP2C phosphatases, SnRK2 kinases, and ABF/AREB transcription factors, thereby regulating plant growth and stress responses. For example, overexpression of *BrLAS* in *A. thaliana* significantly enhances drought tolerance, likely through ABA-mediated pathways [26]. Furthermore, ABA-signaling transcription factors such as ABF/AREB bind to ABA-responsive elements (ABREs), thereby activating the activating the expression of stress-responsive genes [27].

E. sibiricus, a heterologous tetraploid plant, is widely distributed across the Eurasian continent and is characterized by remarkable genetic diversity and strong ecological adaptability [28]. It holds significant value for the establishment of high-yield artificial grasslands, especially in regions such as the Tibetan Plateau and the Northern China. Moreover, *E. sibiricus* significantly contributes to the restoration and improvement of natural grasslands, thereby enhancing ecological quality and increasing grassland productivity [29]. Its high yield and resilience to environmental stresses make it an ideal forage species for promoting sustainable livestock production and grassland ecological restoration. Recently, the reference genome of *E. Sibiricus* was published, facilitated a deeper understanding of its genetic composition and evolutionary history through comprehensive genome-wide and population genomic analyses [30, 31]. This high-quality genomic resource provides a solid scientific foundation for future breeding programs, germplasm improvement, and practical applications, advancing the utilization and development of this important forage crop.

In this study, a systematic genome-wide identification and characterization of *GRAS* transcription factor genes (*EsGRAS*) was conducted in *E. Sibiricus* based on its reference genome. A total of 130 *EsGRAS* genes were identified and analyzed for their chromosomal distribution, gene duplication events, cis-regulatory elements, gene structures, and conserved motifs. Phylogenetic analysis revealed evolutionary relationships between *E. Sibiricus* EsGRAS proteins and *GRAS* homologs from *A. thaliana*, *O. sativa*, *Triticum aestivum*, and *Brachypodium distachyon*. Additionally, expression profiles across various tissues in seedlings and mature plants, as well as under four abiotic stress conditions, provided insights into the functional diversity of *EsGRAS* genes. This systematic analysis demonstrates the potential regulatory roles of *EsGRAS* genes in growth, development and stress responses in *E. Sibiricus*, and offers a valuable genomic resource for future research on this species.

2. Material and methods

2.1 Identification and chromosomal localization of *E. sibiricus GRAS* genes

The genomic data for *E. sibiricus* was obtained from Scientific Data (https://www.nature.com/articles/s41597-024-03622-4 provided on January 6, 2025) [31]. GRAS protein sequences of *A. thaliana* were retrieved from the TAIR database (http://www.arabidopsis.org/). To identifiy *EsGRAS* genes, BLASTp searches were performed in TBtools using *AtGRAS* sequences as queries. Additionally, conserved domain analysis was conducted using the CDD-Search database (https://www.ncbi.nlm.nih.gov/Structure/bwrpsb/bwrpsb.cgi), and additional domain confirmation was carried out through the InterPro database (https://www.ebi.ac.uk/interpro/), allowing differentiation between GRAS-domain and non-GRAS-domain proteins. Pfam model files were downloaded from the Pfam database (https://www.ebi.ac.uk/interpro/download/Pfam/) and used to further confirm the presence of *GRAS* domains (PF03541) within the candidate sequences using TBtools. The chromosomal positions of the identified *EsGRAS* genes was determained based on *E. sibiricus* genome annotation data. Physicochemical properties of the *EsGRAS* proteins, including amino acid length, molecular weight (MW), isoelectric point (PI), instability index, aliphatic index, average hydrophobicity (GRAVY), and predicted subcellular localization, were analyzed using the ExPASy protParam tool (http://web.expasy.org/).

2.2 Phylogenetic analysis of the *EsGRAS* gene family

GRAS amino acids sequences were obtained from multiple databases for *A. thaliana*, *O. sativa*, *B. distachyon*, and *T. aestivum*. These sequences were obtained from TAIR (The *A. thaliana* Information Resource), the Rice Genome Annotation Project, the Sol Genomics Network, and GIGADB (Genomic Data Commons for Agriculture http://www.gigadb.org.) To investigate the evolutionary relationships among the *EsGRAS* gene family members, a comprehensive phylogenetic tree was constructed. For further functional analysis, additional *GRAS* amino acid sequences from the same species were retrieves from NCBI (National Center for Biotechnology Information https://www.ncbi.nlm.nih.gov/), Pear MODB (a molecular database for plant sequences http://www.plantgdb.org/), Plant TFDB (a comprehensive database for plant transcription factors http://planttfdb.gao-lab.org/), and TAIR. The phylogenetic tree was generated using the Neighbor-Joining (NJ) method in MEGA 11.0 with 1,000 bootstrap replications to assess the reliability of the branches. The resulting tree was then visualized using the iTOL online platform (http://itol.embl.de/) to generate a clear and interactive display of phylogenetic relationships.

2.3 Gene structure and multiple sequence alignment analysis

Motif analysis of the EsGRAS proteins was conducted using the MEME tool (http://meme-suite.org/tools/meme) as previously described [32], resulting in the identification of 8 conserved motifs. Additionally, the gene structures, including eron-intron organization and conserved domain distribution of *EsGRAS* family members, were analyzed using TBtools to gain a comprehensive understanding of their structural features.

2.4 Gene duplication and synteny analysis of the *EsGRAS* gene family

The chromosomal location and mapping information for the *EsGRAS* gene family members were obtained from the *E. sibiricus* genome annotation file (GFF3 format) using TBtools. Gene distribution across chromosomes was visualized as described by Chen et al [33]. To investigate syntenic relationships, the

genonmic sequences of *A. thaliana* and *T. aestivum* were downloaded from the Phytozome database (https://phytozome-next.jgi.doe.gov/). Synteny analysis was then performed using the One Step MCScanX function in TBtools, comparing *E. sibiricus* with *A. thaliana* and wheat. Analysis parameters were set to 4 blast hits with an E-value threshold of 1e-10 to ensure accuracy and reliability.

2.5 Identification of cis-acting regulatory elements in the promoters and prediction of protein-protein interactions

To investigate the potential functions and expression regulation mechanisms of the *EsGRAS* genes, the 2000 bp upstream promoter sequences of these genes were extracted and uploaded to NCBI. The PlantCARE database (accessed on January 8, 2025, http://bioinformatics.psb.ugent.be/webtools/plantcare/html/) and TBtools were used for visualization [34]. Protein-protein interaction predictions were carried out using the online STRING database (accessed on January 9, 2025, https://cn.string-db.org/). Interaction protein information was retrieved from UniProt (https://www.uniprot.org/, accessed on January 10, 2025).

2.6 Growth conditions and stress treatments

Plant materials of *E. sibiricus* used in this experiment were provided by the College of Animal Science and Veterinary Medicine at Qinghai University, China. Seedlings were cultivated under controlled condition in an artificial climate chamber at the Institute of Animal Science of the Chinese Academy of Agricultural Sciences in Beijing, China. Hydroponically grown seedlings were maintained under a 16 hours light/8 h dark photoperiod, with day/night temperature of 25°/21°C, a light intensity of 250 μmol photons·m^{-2}·s^{-1}, and a relative humidity of 70%. For abiotic stress treatments, two- week- old seedlings were subjected to salt (200 mM NaCl), drought (20% PEG6000), abscisic acid (ABA, 0.1 mM), and gibberellin (GA, 0.1 mM).Samples were collected at 8 time points: 0 h, 3 h, 6 h, 12 h, 24 h, 48 h, 72 h, and 100 h. All treatments included three biological replicates.

To investigate gene expression patterns across tissues, roots, stems, leaves, and spikes were collected at the heading stage. Additionally, seeds, young roots and two- weeks-old seedlings were sampled for expression analysis. All samples were collected in triplicate ensure experimental reliability. The expression data was visualized using Amazing Heat Map software to generate heatmaps illustrating expression profiles under different conditions.

2.7 Total RNA extraction and qPCR analysis

Total RNA was extracted utilizing the Trizol reagent (Invitrogen, Carlsbad, CA, USA), following the manufacturer's prescribed protocol. Subsequently, genomic DNA contamination was eliminated through DNase digestion employing the services of Promega (Madison, WI, USA). The synthesis of the first-strand cDNA was accomplished using M-MLV reverse transcriptase (also provided by promega) with 1 μg of the total RNA as a template. RT-qPCR analysis was performed on the CFX96 Touch™ Real-Time PCR Detection System from Bio-Rad (Hercules, CA, USA). The PCR amplification parameters were set as: an initial denaturation at 95°C for 2 minutes, followed by 40 cycles of denaturation at 95°C for 15 seconds and annealing/extension at 60°C for 40 seconds. A final cycle consisted of denaturation at 95°C for 15 seconds and annealing/extension at 60°C for 15 seconds. The alfalfa actin gene was utilized as the internal reference, and relative gene expression was analyzed using the 2^-ΔΔCt methodology. All experimental procedures were repeated with three biological replicates and three technical replicates to ensure reliability. Primer design was done using Primer 5.0 software for accurate and consistent results.

2.8 Data analysis

The statistical analysis was conducted utilizing the one-way analysis of variance (ANOVA) within the SPSS software version 23.0. The data was presented in the form of mean values accompanied by their corresponding standard deviations. Graphs were created and thoroughly analyzed using GraphPad Prism 10.1.1 software. Any observed differences were deemed statistically significant when the P-value was below 0.05.

3. Results

3.1 Genome-wide identification of the *GRAS* gene family in *E. sibiricus*

Atotal of 130 candidate *EsGRAS* genes were identified in the *E. sibiricus* genome using comparative genomics techniques [31]. These genes were named according to their sequence homology with *A. thaliana* GRAS proteins. The key characteristics of the *EsGRAS* gene family —including TIGR loci, chromosomal locations, coding sequence lengths, molecular weights, theoretical isoelectric points, instability indices, aliphatic indices, and the hydrophilicity—are summarized in Table 1. The lengths of EsGRAS proteins vary substantially, ranging from 104 to 1,457 amino acid residues, with molecular weight spanning from 12.07kD to 163.40kDa. The theoretical isoelectric points (pI) value range from 4.75 to 9.43, while instability indices vary between 30.90 and 71.21, indicating that the thermal stability range of these proteins in vitro. Furthermore, the aliphatic index ranges from 64.05 to 105.80, reflecting variation in thermostability. Most EsGRAS proteins have negative GRAVY (Grand Average of Hydropathy) scores, indicating a predominantly hydrophilic nature, However, several members (e.g., *EsGRAS1, EsGRAS10, EsGRAS12, EsGRAS17, EsGRAS28, EsGRAS29, EsGRAS30, EsGRAS32, EsGRAS33, EsGRAS34, EsGRAS38, EsGRAS41, EsGRAS80, EsGRAS92, EsGRAS93*, and *EsGRAS100*) exhibit positive GRAVY scores, indicating hydrophobicity. Subcellular localization predictions revealed that the majority of *EsGRAS* members are localized to the nucleus, cytoplasmic, and chloroplast, while a minority are predicted to localize to theperoxisome, mitochondrial, cytoskeleton, endoplasmic reticulum, or extracellular space.

Table 1
List and detailed information of identified *GRAS* genes in *E.sibiricus*.

Gene Name	Gene ID	Chr	CDS Length	Pep Length	Molecular Weight(kDa)	Theoretical pI	Instability Index	Aliphatic Index	Grand Average of Hydropathicity	Subcellula localizatio prediction
EsGRAS1	evm.model.Chr01.7082	1	1377	458	49,656.73	5.38	36.95	93.14	0.09	Chloroplas
EsGRAS2	evm.model.Chr01.7190	1	1794	597	64,089.63	5.58	63.19	64.37	-0.41	Nuclear
EsGRAS3	evm.model.Chr01.7423	1	1674	557	61,462.41	5.84	47.64	77.59	-0.35	Chloroplas
EsGRAS4	evm.model.Chr01.7755	1	1311	436	47,820.45	6.16	54.79	91.61	-0.19	Nuclear
EsGRAS5	evm.model.Chr01.8450	1	1713	570	64,265.05	5.94	40.42	83.53	-0.44	Cytoplasm
EsGRAS6	evm.model.Chr01.18120	1	1893	630	66,501.02	6.29	51.54	85.48	-0.14	Nuclear
EsGRAS7	evm.model.Chr01.19209	1	1500	499	52,711.86	5.48	37.98	80.90	-0.25	Nuclear
EsGRAS8	evm.model.Chr01.20585	1	1536	511	54,059.03	6.41	51.76	84.36	-0.15	Nuclear
EsGRAS9	evm.model.Chr01.22082	1	1452	483	52,884.66	6.00	40.54	98.28	-0.05	Mitochon
EsGRAS10	evm.model.Chr01.22106	1	1401	466	50,724.47	6.28	43.39	95.41	0.06	Chloroplas
EsGRAS11	evm.model.Chr02.4465	2	2142	713	77,164.08	6.03	60.66	78.53	-0.25	Nuclear
EsGRAS12	evm.model.Chr02.7906	2	1380	459	49,652.70	5.44	38.36	92.09	0.09	Chloroplas
EsGRAS13	evm.model.Chr02.7979	2	1794	597	63,939.47	5.58	62.44	64.05	-0.40	Nuclear
EsGRAS14	evm.model.Chr02.8105	2	1665	554	61,260.37	5.97	47.65	78.72	-0.34	Chloroplas
EsGRAS15	evm.model.Chr02.8519	2	1311	436	47,604.31	6.50	50.87	93.44	-0.17	Cytoplasm
EsGRAS16	evm.model.Chr02.8983	2	1713	570	64,363.03	5.98	40.78	82.33	-0.47	Cytoplasm
EsGRAS17	evm.model.Chr02.17520	2	1251	416	45,472.07	5.93	49.23	97.04	0.02	Cytoplasm
EsGRAS18	evm.model.Chr02.19199	2	2145	714	75,247.41	6.78	53.15	88.85	-0.06	Chloroplas
EsGRAS19	evm.model.Chr02.20403	2	1521	506	53,973.08	6.93	55.35	83.85	-0.16	Nuclear
EsGRAS20	evm.model.Chr02.21979	2	1429	475	52,511.29	6.07	42.90	99.31	-0.02	Cytoplasm
EsGRAS21	evm.model.Chr02.21980	2	1113	370	41,061.08	6.32	47.09	95.54	-0.14	Cytoplasm
EsGRAS22	evm.model.Chr02.21995	2	1464	487	53,347.00	5.66	44.69	91.48	-0.06	Cytoplasm
EsGRAS23	evm.model.Chr02.21996	2	1464	487	53,347.00	5.66	44.69	91.48	-0.06	Cytoplasm
EsGRAS24	evm.model.Chr02.21999	2	1737	578	62,525.29	6.19	46.18	85.19	-0.11	Mitochon
EsGRAS25	evm.model.Chr03.2227	3	2280	759	86,455.02	8.33	46.12	74.22	-0.53	Nuclear
EsGRAS26	evm.model.Chr03.2230	3	1689	562	63,805.31	5.97	48.01	81.25	-0.41	Cytoplasm
EsGRAS27	evm.model.Chr03.2232	3	2373	790	89,478.48	9.43	65.35	82.01	-0.52	Nuclear
EsGRAS28	evm.model.Chr03.11804	3	1866	621	65,087.02	5.96	53.43	82.05	0.02	Cytoplasm
EsGRAS29	evm.model.Chr03.14314	3	675	224	24,328.38	7.76	41.66	105.80	0.39	Cytoplasm
EsGRAS30	evm.model.Chr03.14850	3	1428	475	50,325.14	5.87	46.97	85.31	0.05	Peroxisom
EsGRAS31	evm.model.Chr03.15332	3	1248	415	44,525.58	6.03	48.51	87.25	-0.11	Cytoplasm
EsGRAS32	evm.model.Chr03.17157	3	696	231	25,171.91	6.23	40.18	88.31	0.10	Chloroplas
EsGRAS33	evm.model.Chr03.17158	3	943	313	32,651.78	6.10	39.87	81.69	0.00	Chloroplas
EsGRAS34	evm.model.Chr03.18852	3	1461	486	51,260.26	6.06	41.36	83.93	0.08	Nuclear
EsGRAS35	evm.model.Chr04.2319	4	2148	715	81,129.01	7.30	48.75	79.44	-0.48	Nuclear
EsGRAS36	evm.model.Chr04.2320	4	2355	784	88,747.40	8.74	51.09	82.90	-0.38	Nuclear
EsGRAS37	evm.model.Chr04.2324	4	1503	500	57,455.36	9.40	51.31	82.74	-0.41	Cytoplasm
EsGRAS38	evm.model.Chr04.11750	4	1863	620	64,885.86	5.93	52.12	80.94	0.02	Nuclear
EsGRAS39	evm.model.Chr04.14998	4	1473	490	51,989.91	5.94	48.47	82.49	-0.01	Peroxisom
EsGRAS40	evm.model.Chr04.15498	4	1239	412	44,196.20	6.02	46.59	87.65	-0.10	Cytoplasm

Gene Name	Gene ID	Chr	CDS Length	Pep Length	Molecular Weight(kDa)	Theoretical pI	Instability Index	Aliphatic Index	Grand Average of Hydropathicity	Subcellula localizatio prediction
EsGRAS41	evm.model.Chr04.19365	4	1479	492	51,927.15	5.62	42.37	85.87	0.12	Nuclear
EsGRAS42	evm.model.Chr05.11883	5	1500	502	52,942.52	5.16	45.91	82.21	-0.01	Nuclear
EsGRAS43	evm.model.Chr05.21261	5	2175	724	81,837.56	8.92	46.24	83.77	-0.45	Nuclear
EsGRAS44	evm.model.Chr05.21264	5	1584	527	60,440.33	5.38	42.12	76.57	-0.56	Nuclear
EsGRAS45	evm.model.Chr05.2854	5	1353	450	48,994.71	6.22	53.11	90.84	-0.12	Nuclear
EsGRAS46	evm.model.Chr05.5649	5	1659	552	61,424.07	4.75	39.69	78.17	-0.29	Nuclear
EsGRAS47	evm.model.Chr05.6228	5	1551	516	56,257.77	5.62	45.15	79.50	-0.18	Cytoplasm
EsGRAS48	evm.model.Chr05.6232	5	1551	516	55,965.61	5.89	42.67	84.22	-0.12	Cytoplasm
EsGRAS49	evm.model.Chr05.7172.2	5	2688	895	97,685.54	6.01	51.46	77.37	-0.34	Nuclear
EsGRAS50	evm.model.Chr06.1025	6	1440	479	54,062.67	6.56	37.50	82.92	-0.43	Cytoplasm
EsGRAS51	evm.model.Chr06.3708	6	1590	529	57,699.75	6.45	52.19	90.40	-0.13	Chloroplas
EsGRAS52	evm.model.Chr06.6611	6	1659	552	61,335.92	4.75	38.69	77.81	-0.28	Nuclear
EsGRAS53	evm.model.Chr06.7185	6	1551	516	56,200.88	5.70	47.19	81.76	-0.13	Nuclear
EsGRAS54	evm.model.Chr06.7186	6	1548	515	55,930.49	5.90	42.85	83.05	-0.15	Cytoplasm
EsGRAS55	evm.model.Chr06.8224	6	2445	814	89,266.95	5.63	50.15	76.66	-0.32	Nuclear
EsGRAS56	evm.model.Chr06.20965	6	1848	616	69,787.53	8.42	47.23	80.10	-0.49	Nuclear
EsGRAS57	evm.model.Chr06.20966	6	1497	498	57,418.28	5.81	38.20	86.85	-0.52	Cytoplasm
EsGRAS58	evm.model.Chr06.20967	6	2124	707	80,343.45	7.23	42.91	83.03	-0.44	Nuclear
EsGRAS59	evm.model.Chr07.301	7	492	163	17,775.59	5.71	59.82	101.23	-0.09	Extracellu
EsGRAS60	evm.model.Chr07.302	7	840	279	31,555.91	6.51	38.73	90.82	-0.16	cytoskelet
EsGRAS61	evm.model.Chr07.310	7	864	287	31,435.22	5.08	54.96	78.22	-0.42	Cytoplasm
EsGRAS62	evm.model.Chr07.792	7	1629	542	57,453.04	5.83	71.21	81.66	-0.19	Chloroplas
EsGRAS63	evm.model.Chr07.2436	7	1866	621	65,669.57	6.23	49.29	74.35	-0.25	Chloroplas
EsGRAS64	evm.model.Chr07.6241	7	2226	741	81,381.48	5.05	41.97	72.75	-0.42	Chloroplas
EsGRAS65	evm.model.Chr07.17266	7	1281	426	45,104.05	6.51	45.11	92.28	-0.01	Nuclear
EsGRAS66	evm.model.Chr08.538	8	768	255	28,993.13	6.54	47.96	91.02	-0.30	Cytoplasm
EsGRAS67	evm.model.Chr08.539	8	315	104	12,074.99	7.83	30.90	88.08	-0.30	Cytoplasm
EsGRAS68	evm.model.Chr08.797	8	1626	541	56,840.37	5.97	64.64	83.84	-0.09	Chloroplas
EsGRAS69	evm.model.Chr08.2682	8	1872	623	65,848.93	6.16	45.14	74.43	-0.22	Chloroplas
EsGRAS70	evm.model.Chr08.6673	8	2202	733	80,848.92	5.08	43.98	73.41	-0.43	Chloroplas
EsGRAS71	evm.model.Chr08.16445	8	1281	426	45,121.13	6.93	45.18	92.51	-0.02	Nuclear
EsGRAS72	evm.model.Chr09.687	9	1842	613	68,589.89	6.84	33.90	78.94	-0.44	Cytoplasm
EsGRAS73	evm.model.Chr09.4174	9	2235	744	81,957.41	5.37	50.29	78.17	-0.41	Cytoplasm
EsGRAS74	evm.model.Chr09.7976	9	1688	555	61,090.27	7.34	54.21	80.13	-0.29	Mitochon
EsGRAS75	evm.model.Chr09.8244	9	2331	776	87,199.61	6.76	50.86	79.43	-0.47	Nuclear
EsGRAS76	evm.model.Chr09.8603	9	1944	647	69,098.49	6.09	57.06	89.00	-0.13	Chloroplas
EsGRAS77	evm.model.Chr09.15553	9	2619	872	99,598.47	9.21	48.73	68.76	-0.80	Cytoplasm
EsGRAS78	evm.model.Chr09.15558	9	2154	717	80,081.80	6.03	40.40	100.54	-0.04	Cytoplasm
EsGRAS79	evm.model.Chr09.18506	9	1653	550	61,014.79	5.78	48.64	83.00	-0.27	Nuclear
EsGRAS80	evm.model.Chr09.20602	9	762	253	26,684.72	8.81	54.37	86.48	0.15	Cytoplasm
EsGRAS81	evm.model.Chr09.21006	9	2238	745	83,316.41	8.06	55.23	74.16	-0.50	Nuclear
EsGRAS82	evm.model.Chr09.23497	9	1938	645	72,684.22	6.21	52.11	78.82	-0.33	Cytoplasm

Gene Name	Gene ID	Chr	CDS Length	Pep Length	Molecular Weight(kDa)	Theoretical pI	Instability Index	Aliphatic Index	Grand Average of Hydropathicity	Subcellula localizatio prediction
EsGRAS83	evm.model.Chr10.4059	10	2232	743	81,921.31	5.26	51.54	78.02	-0.43	Cytoplasm
EsGRAS84	evm.model.Chr10.8058	10	1533	510	55,925.26	6.75	53.32	81.47	-0.26	Nuclear
EsGRAS85	evm.model.Chr10.8198	10	2332	777	87,100.55	7.06	52.21	78.58	-0.48	Nuclear
EsGRAS86	evm.model.Chr10.8413	10	1947	648	69,326.70	6.12	56.99	88.84	-0.14	Chloroplas
EsGRAS87	evm.model.Chr10.15554	10	3745	1247	140,279.68	7.85	43.14	94.60	-0.18	Nuclear
EsGRAS88	evm.model.Chr10.15580	10	4374	1457	163,397.12	6.91	41.48	96.62	-0.09	Cytoplasm
EsGRAS89	evm.model.Chr10.18541	10	1650	549	60,790.65	5.75	48.66	84.23	-0.25	Nuclear
EsGRAS90	evm.model.Chr10.21058	10	1938	645	71,993.53	6.03	53.78	77.33	-0.36	Nuclear
EsGRAS91	evm.model.Chr11.13918	11	2124	707	73,958.89	5.96	48.86	85.19	-0.02	Nuclear
EsGRAS92	evm.model.Chr11.7841	11	1188	395	41,432.86	5.45	48.85	91.16	0.03	Cytoplasm
EsGRAS93	evm.model.Chr12.7936	12	1194	397	41,756.17	5.51	47.25	89.72	0.00	Cytoplasm
EsGRAS94	evm.model.Chr12.14920	12	1689	562	59,783.11	5.13	43.47	76.09	-0.15	Nuclear
EsGRAS95	evm.model.Chr12.17171	12	1590	529	58,652.87	5.76	51.21	79.85	-0.28	Nuclear
EsGRAS96	evm.model.Chr12.20835	12	1902	633	67,251.31	6.03	50.67	85.85	-0.11	Chloroplas
EsGRAS97	evm.model.Chr12.20909	12	3210	1069	119,747.38	5.69	50.83	70.16	-0.53	Nuclear
EsGRAS98	evm.model.Chr13.1397	13	1954	617	64,950.90	5.00	51.31	78.40	-0.15	Nuclear
EsGRAS99	evm.model.Chr13.1772	13	1662	553	59,140.81	4.91	51.88	84.07	-0.03	Chloroplas
EsGRAS100	evm.model.Chr13.4018	13	1422	473	52,081.01	5.00	42.84	89.51	0.00	Nuclear
EsGRAS101	evm.model.Chr13.4444	13	2034	677	72,099.74	5.94	58.15	89.76	-0.15	Nuclear
EsGRAS102	evm.model.Chr13.4664	13	1386	461	51,964.96	6.85	49.29	95.66	-0.14	Cytoplasm
EsGRAS103	evm.model.Chr13.5327	13	2433	810	89,069.16	5.94	41.10	71.00	-0.41	Peroxisom
EsGRAS104	evm.model.Chr13.5332	13	2034	677	74,745.80	6.44	53.93	81.33	-0.40	Nuclear
EsGRAS105	evm.model.Chr13.5347	13	2022	673	75,059.17	5.64	49.74	82.67	-0.38	Cytoplasm
EsGRAS106	evm.model.Chr13.5348	13	1794	597	67,243.38	5.98	41.45	79.43	-0.34	Cytoplasm
EsGRAS107	evm.model.Chr13.5349	13	1764	587	66,531.60	5.92	39.33	81.62	-0.38	Chloroplas
EsGRAS108	evm.model.Chr13.5350	13	1908	635	71,239.02	5.25	38.95	81.28	-0.36	Cytoplasm
EsGRAS109	evm.model.Chr13.5351	13	1938	645	72,219.26	6.13	41.10	83.21	-0.31	Endoplasm reticulum
EsGRAS110	evm.model.Chr13.5363	13	1935	644	72,383.69	6.15	50.29	79.44	-0.35	Cytoplasm
EsGRAS111	evm.model.Chr13.5364	13	1791	596	67,695.12	6.61	44.43	78.56	-0.38	Cytoplasm
EsGRAS112	evm.model.Chr13.11647	13	2094	697	73,337.31	5.96	46.54	86.96	-0.02	Nuclear
EsGRAS113	evm.model.Chr14.2718	14	1857	618	64,996.03	5.06	49.81	79.05	-0.13	Nuclear
EsGRAS114	evm.model.Chr14.3195	14	1650	549	59,034.80	4.88	53.80	84.99	-0.03	Chloroplas
EsGRAS115	evm.model.Chr14.5637	14	1356	451	49,492.96	5.07	44.52	89.76	-0.04	Cytoplasm
EsGRAS116	evm.model.Chr14.6237	14	2043	680	72,317.85	5.97	58.87	89.66	-0.17	Nuclear
EsGRAS117	evm.model.Chr14.6412	14	1341	446	50,159.74	6.32	48.85	92.98	-0.18	Cytoplasm
EsGRAS118	evm.model.Chr14.6748	14	1791	596	67,580.02	6.73	43.74	80.37	-0.34	Cytoplasm
EsGRAS119	evm.model.Chr14.6749	14	1935	644	72,265.53	6.21	48.81	80.33	-0.32	Nuclear
EsGRAS120	evm.model.Chr14.6760	14	1950	649	73,000.15	5.79	45.06	82.54	-0.32	Cytoplasm
EsGRAS121	evm.model.Chr14.6761	14	1059	352	40,175.16	8.47	43.50	81.73	-0.23	Chloroplas
EsGRAS122	evm.model.Chr14.6762	14	1770	589	66,718.60	6.05	37.41	81.04	-0.41	Chloroplas
EsGRAS123	evm.model.Chr14.6763	14	1767	588	66,323.40	5.63	41.52	79.47	-0.33	Cytoplasm

Gene Name	Gene ID	Chr	CDS Length	Pep Length	Molecular Weight(kDa)	Theoretical pI	Instability Index	Aliphatic Index	Grand Average of Hydropathicity	Subcellula localizatic prediction
EsGRAS124	evm.model.Chr14.6764	14	1740	579	63,438.20	5.82	55.25	80.45	-0.28	Nuclear
EsGRAS125	evm.model.Chr14.6765	14	2019	672	74,731.74	6.20	53.68	80.89	-0.42	Cytoplasm
EsGRAS126	evm.model.Chr14.6766	14	2445	814	89,284.53	5.97	39.52	70.76	-0.41	Peroxisom
EsGRAS127	evm.model.Chr14.13211	14	1686	561	59,870.24	5.23	42.88	76.06	-0.18	Nuclear
EsGRAS128	evm.model.Chr14.15240	14	1611	536	59,488.79	6.02	50.40	78.82	-0.33	Nuclear
EsGRAS129	evm.model.Chr14.17606	14	1932	643	71,926.81	5.50	46.77	82.10	-0.28	Cytoplasm
EsGRAS130	evm.model.Chr14.18646	14	1917	638	67,437.57	5.98	51.00	87.19	-0.08	Cytoplasm

3.2 Phylogenetic tree analysis of the *GRAS* gene family in *E. sibiricus*

To explore the evolutionary relationships of GRAS proteins in *E. sibiricus*, a comprehensive phylogenetic analysis was conducted using GRAS protein sequences from four model plants speciesincluding *A. thaliana*, *O. sativa, B. distachyon*, and *T. aestivum*. (Fig. 1). To further explore the structural complexity of *GRAS* gene family, a Neighbor-Joining (NJ) phylogenetic tree was constructed based on protein sequences of 130 *EsGRAS*, 34*AtGRAS*, 60 *OsGRAS*, 78 *BdGRAS* and 121 *TaGRAST.* The resulting phylogenetic tree classified these GRAS proteins into eleven distinct clades, revealing conserved and divergent evolutionary patterns across species. Notably, many *EsGRAS* members clustered closely with *TaGRAS* genes from wheat, indicating a strong co-evolutionary relationship between *E. sibiricus* and *T. aestivum*. Specifically, in the DELLA subfamily, for instance, *EsGRAS7*, *EsGRAS82*, and *EsGRAS97* exhibit high sequence similarity with wheat *GRAS* genes, such as *TaGRAS43*, *TaGRAS18*, *TaGRAS99*, and *TaGRAS66*, suggesting potential conservation of function and evolutionary significance. Moreover, the analysis reveals a significant expansion of the *GRAS* gene family from lower to higher plants, likely driven by extensive gene duplication events. This expansion may have contributed to the evolutionary success of terrestrial plants by facilitating adaptive modifications in traits such as plant height in response to diverse environmental conditions [35].

3.3 Gene structure analysis of the *GRAS* gene family in *E. sibiricus*

To further investigate the functional diversity of *GRAS*-associated candidate genes in *E. sibiricus*, conserved motifs, domains, and gene structures were analyzed (Fig. 2). Motif analysis using the MEME Suite enabled the identification of conserved sequence elements associated with the *GRAS* domain. This approach facilitated the comprehensive assessment of the sequence conservation among homologous domains s, particularly in relation to the core *GRAS* region. Eight conserved motifs were detected across GRAS proteins, with Motif 8 showing the highest degree conservation. The PAT1 subfamily exhibited a relatively stable motif pattern, with most members displaying minimal motif loss. In contrast, other subfamily members displayed substantial variation, including the absence of specific motifs, which may underlie functional divergence among *GRAS* subgroups (Fig. 2A). All *EsGRAS*-encoded proteins contain the conserved core *GRAS* domain (Fig. 2B). Notably, several members possess additional functional domains: *EsGRAS87* and *EsGRAS88* contain additional Rx-N and NB-ARC domains; *EsGRAS103* and *EsGRAS126* contain an extra SSP160 domain; *EsGRAS27* possess a Peptidase-C48 domain; *EsGRAS38* contain a PHA03378 domain; *EsGRAS77* contain a PLN02983 domain, *EsGRAS78* possess an Rx-N domain, *EsGRAS97* contain a PMD domain, and*EsGRAS98* and *EsGRAS113* (both from the DELLA subfamily) harbor additional DELLA domains. Intron-exon structure analysis revealed that the number of introns among *EsGRAS* genes varies from 1 to 9, with a maximum of five exons oserved (Fig. 2C). Collectively, these findings provide critical insights into the structural conservation and functional diversification of candidate *GRAS* genes in *E. sibiricus*. The presence of both conserved and subfamily-specific domains, and gene structures suggests their involvement in diverse biological processes, highlighting their evolutionary significance and regulatory potential.

3.4 Chromosomal location and synteny analysis

The chromosomal distribution of *EsGRAS* genes in *E. sibiricus* was determined by mapping the open reading frames (ORFs) of all identified *EsGRAS* genes to the reference genome (Fig. 3A). The *EsGRAS* genes were unevenly distributed across the 14 chromosomes. Specifically, chromosome 14 harbored the highest number of *GRAS* genes(18), followed by chromosome 13 with 15 genes, chromosome 2 with 14 genes, chromosome 9 with 11 genes, and chromosomes 1 and 3 (10 each). Chromosome 6 contained 9 genes, chromosomes 5 and 10 each had 8 genes. Chromosomes 4 and 7 contain 7 each, chromosome 8 had 6, chromosome 12 had 5 genes, and chromosome 11 had the fewest, with only 2 genes. Intraspecific synteny analysis identified 41 collinear gene pairs within *E. sibiricus* (Fig. 3B), demonstrating that a large proportion of *EsGRAS* genes are organized in tandem arrays. This pattern is likely attributable to the allopolyploid nature of *EsGRAS*, which promotes the retention of duplicated gene srgments. To further elucidate the evolutionary relationships of the *EsGRAS* gene family, a comparative synteny map was constructed among *A. thaliana*, *E. sibiricus*, and *T. aestivum* (Fig. 3C; Supplementary Fig. S1). Interestingly, *E. sibiricus* shares only one orthologous gene pairs with *A. thaliana*, whereas shares as many as 88 orthologous gene pairs with wheat. These results indicated a closer evolutionary relationship between *E. sibiricus* and *T. aestivum*, consistent with their shared evolutionary lineage and higher sequence similarity.

3.5 Protein-protein interaction network analysis of the *GRAS* gene family in *E. sibiricus*

To explore the potential functional associations of EsGRAS proteins, a protein-protein interaction (PPI) network was constructed using STRING database. The analysis revealed a complex interaction landscape, suggesting that *GRAS* family proteins are involved in diverse biological processes, including plant hormone signaling, environmental stress responses, and developmental regulation (Fig. 4). The resulting network comprised 92 highly interconnected genes within the *GRAS* family. Structurally, the network was organized into concentric layers: the inner two circles contained four *EsGRAS* genes and nine indirectly associated genes/transcription factors; the third circle included four additional *EsGRAS* genes and 25 interacting genes; and the outermost layer contained 14 *EsGRAS* genes along with 36 indirectly interacting genes or transcription factors. the first and second circles encompass Key regulatory proteins such as

GID1, GA2OX, GA3OX, PAT1, PHYA, and NSP2 were centrally positioned within the network, indicating their prominent roles in *GRAS*-mediated pathways. Transcription factors like SOC1 and MOC1 were also integrated into the the interaction network, further supporting the regulatory diversity of EsGRAS proteins. These findings suggest that *EsGRAS* genes and their interacting patners may share conserved domains that facilitate functional crosstalk and coregulation. Overall, this network analysis provides valuable insights into the functional roles and interaction dynamics of the *GRAS* gene family in *E. sibiricus*, offering a comprehensive perspective on their intricate interactions and roles in biological processes, laying a foundation for future functional genomics studies.

3.6 Identification of cis-acting regulatory elements in the promoters of the *GRAS* gene family in *E.sibiricus*

Using Plant CARE database, cis-acting regulatory elements in 2000 bp upstream promoter regions of *EsGRAS* genes were identified. A total of 3,499 cis-elements were detected across the *EsGRAS* promoters (Fig. 5B). Among them, 1,565 were associated with hormone response regulation (Fig. 5C). Six types of hormone-responsive motifs were detected: abscisic acid responsive elements (ABRE), methyl jasmonate response elements (CGTCA-motif and TGACG-motif), salicylic acid response elements (TCA-element), and gibberellin response elements (P-box and GARE-motif). Additionally, various stress-responsive elements were identified including drought-inducible elements (MBS), low-temperature response elements (LTR), anaerobic response elements (ARE), and defense and stress response elements (TC-rich repeats) etc. These cis-acting regulatory elements were classified into four major categories: (1) environmental stress response elements, (2) hormone response elements, (3) development-related elements, and (4) light response elements (Fig. 5B). Among the environmental stress response elements, AREs were the most abundant, accounting for 33.1% of the total. Within the hormone response category, ABRE motif were dominant, comprising 46.2%, followed by CGTCA-motif and TGACG-motif at 20.4% and 20.3%, respectively. For five development-related elements, the CAT-box element, linked to meristem expression, represented 52.8%, followed by the O2-site, a cis-element involved in zein metabolism regulation, at28.9%. For light-responsive elements, the G-box was the most prevalent (51.8%), followed by the Box-4 motif (15.1%) (Fig. 5B). Notably, the distribution of cis-acting regulatory elements was gene-specific. For instance, *EsGRAS94* contains highest number of environmental stress-response motifs, whereas *EsGRAS51* and *EsGRAS58* were enriched with hormone-responsive elements. *EsGRAS111*, *EsGRAS125*, and *EsGRAS87* exhibited higher proportions of development-related elements. *EsGRAS10* showed a notable enrichment in light-responsive elements (Fig. 5C). This diverse distribution suggests functional specialization of *EsGRAS* genes in response to various environmental cues and developmental processes.

3.7 Tissue-specific expression of *GRAS* candidate genes in *E. sibiricus*

To investigate the potential biological functions of *GRAS* candidate genes in different tissues of *E. sibiricus*, and to determine whether these genes serve as general regulators or participate in tissue-specific developmental pathways regulatory mechanisms, a comprehensive tissue-specific expression analysis was performed (Fig. 6). The results revealed distinct spatial expression patterns among various *EsGRAS* genes. For example, *EsGRAS104* exhibited strong expression in root tissues, suggesting a possible role in root development or nutrient uptake. *EsGRAS46* and *EsGRAS77* showed high transcript level in stems, while *EsGRAS117* demonstrated elevated expression in leaves, indicating involvement in aerial organ differentiation or photosynthetic regulation. A number of genes, including *EsGRAS6, EsGRAS12, EsGRAS24, EsGRAS34, EsGRAS56*, *EsGRAS57*, *EsGRAS64*, *EsGRAS78*, *EsGRAS103*, *EsGRAS116*, *EsGRAS121*, and *EsGRAS130*, displayed predominant expression levels in spike tissues, implicating them in reproductive development or floral morphogenesis. Notably, several *EsGRAS* members (*EsGRAS8, EsGRAS16, EsGRAS50, EsGRAS72, EsGRAS75*, and *EsGRAS95*) showed predominant expression in seedlings, highlighting their potential role during early growth stages. Similarly, *EsGRAS14, EsGRAS41, EsGRAS71*, and *EsGRAS74* were enriched in young roots, whereas *EsGRAS4*, *EsGRAS13, EsGRAS15, EsGRAS36, EsGRAS49, EsGRAS107*, and *EsGRAS111* were highly expressed in seeds, suggesting involvement in seed development or dormancy regulation. Notably, consistent with observations in wheat and other cereal crops, most *GRAS* genes exhibited elevated expression in the seedling, indicated that *GRAS* family genes in *E. sibiricus* may play a conserved and crucial regulatory roles during plant early development stages.

3.8 Expression of GRAS candidate genes in E. sibiricus in response to salt, drought, ABA, and GA stress

To assess the involvement of *GRAS* genes in the stress response, their expression profiles were examined under salt, drought, abscisic acid (ABA), and gibberellin (GA) treatments. Two-week-old *E. sibiricus* plants were hydroponically treated with 200 mM NaCl (salt stress), 20% PEG6000 (drought stress), 0.1 mM abscisic acid (ABA), or 0.1 mM GA for up to 100 hours. Samples were collected at 3, 6, 12, 24, 48, 72, and 100 hours post-treatment. For each treatment and time point, three biological replicates were analyzed using qRT-PCR technology to quatify gene expression dynamics. Under salt stress condition, the majority of *GRAS* genes exhibited a gradual downregulation trend over time. However, a subset of genes—*EsGRAS5*, *EsGRAS11*, *EsGRAS37*, *EsGRAS98*, and *EsGRAS114*—initially showed increased expression, followed by a decline. Notably, *EsGRAS5*, *EsGRAS11*, and *EsGRAS37*, all members of the SHR subfamily, displayed a consistent expression pattern during salt stress, suggesting a shared regulatory mechanism. Among these, *EsGRAS128* exhibited the most pronounced induction, with expression levels increasing up to 4.8-fold (Fig. 7), indicating its potential role as a positive regulator in salt stress responses and represents a promising candidate for future studies on salt adaptation mechanisms. Drought stress elicited a distinct expression pattern, with many *GRAS* genes displayed early upregulation followed by a progressive decline. Specifically, Genes such as *EsGRAS37*, *EsGRAS45*, *EsGRAS80*, *EsGRAS111*, *EsGRAS128*, *EsGRAS90*, and *EsGRAS95* were significantly induced during the early stages of drought exposure. Particularly, *EsGREAS90* and *EsGRAS95* showed substantial expression increases, reaching 8.5-fold and 10.5-fold, respectively (Fig. 7). These observations demonstrated that these genes may contribute to osmotic stress adaptation and root developmental regulation under drought conditions.

Together, these findings underscore the critical roles of *GRAS* gene family members in modulating abiotic stress responses in *E. sibiricus*, and highlight specific candidates such as *EsGRAS128*, *EsGRAS90*, and *EsGRAS95* for further functional characterization in stress-resilience pathways.

Under ABA treatment, multiple *EsGRAS* genes—including *EsGRAS14*, *EsGRAS45*, *EsGRAS80*, *EsGRAS83*, *EsGRAS84*, *EsGRAS93*, *EsGRAS98*, *EsGRAS108*, *EsGRAS118*, and *EsGRAS113*—displayed transient upregulation followed by a subsequent decline (Fig. 8). Notably, *EsGRAS5* and *EsGRAS120* showed

significant and sustained induction, with transcription levels increasing by 4.9-fold and 9.6-fold, respectively, compared to per-treatment expression levels. Intriguingly, induction pattern of *EsGRAS95* under ABA treatment was consistent with its response to drought stress, suggesting a possible role of *GRAS* genes in ABA-dependent stress signaling pathways. GA regulates a broad range of plant growth and developmental processes, including stem elongation, tillering, and floral organ development. Under GA treatment, several *EsGRAS* genes—including *EsGRAS5*, *EsGRAS8*, *EsGRAS22*, *EsGRAS24*, *EsGRAS45*, *EsGRAS99*, and *EsGRAS100*—exhibited significant downregulation relative to pre-treatment levels. In contrast, *EsGRAS113* expressed a marked upregulation,with transcription levels increasing by 2.1-fold (Fig. 8). These differential expression patterns indicated that *GRAS* family members in *E. sibiricus* likely play diverse roles in GA signaling transduction. Collectively, the results underscore the involvement of *EsGRAS* genes in gibberellin-responsive pathways, reinforcing their functional significance in regulating plant growth and stress adaptation.

4. Discussion

In this study, a total of 130 *GRAS* transcription factor genes were identified from *E. sibiricus* genome and categorized into eleven distinct groups based on phylogenetic relationships. Comparative genomic analysis demonstrated that the *GRAS* gene family reveals exhibits substantial variation in copy number across different species, with 34 members reported in *A. thaliana* [36], 48 in *Brachypodium distachyon* [37], 55 in *Melilotus albus* [38], 55 in *Medicago sativa* [39], and 62 in *Hordeum vulgare* [40]. Despite species-specific differences in gene number, the overall structure features and motif compositions of of *EsGRAS* genes were largely conserved. All *EsGRAS* proteins contained the characteristic *GRAS* domain, and two members *EsGRAS*98 and *EsGRAS113* additionally possessed a DELLA domain, consistent with previous reports in monocots and dicots [41].

Gene duplication is recognized as a primary mechanism driving the expression and diversification of transcription factor families in plants [42]. In *E. sibiricus*, the *GRAS* gene family comprises both single-copy and multicopy genes. Multiple members, including *EsGRAS2*, *EsGRAS4*, *EsGRAS5*, *EsGRAS22*, *EsGRAS30*, *EsGRAS46*, *EsGRAS51*, *EsGRAS53*, *EsGRAS55*, *EsGRAS63*, *EsGRAS91*, *EsGRAS94*, *EsGRAS101*, *EsGRAS109*, *EsGRAS110*, *EsGRAS114*, and *EsGRAS118*, exhibit gene duplication events and are conserved across other plant species, suggesting that they have undergone evolutionary retention due to functional significance. Chromosomal mapping of *EsGRAS* genes revealed a non-random distribution pattern, with multiple members located in distinct chromosomal regions (Fig. 3). This uneven distribution implies the occurrence of large-scale genomic events such as whole-genome duplication (WGD) and segmental duplication. Based on synteny and gene collinearity analysis, the majority of *EsGRAS* genes appear to have originated from WGD events, whereas a subset genes—such as *EsGRAS3*, *EsGRAS7*, *EsGRAS12*, *EsGRAS17*, *EsGRAS22*, *EsGRAS31*, *EsGRAS35*, *EsGRAS37*, *EsGRAS42*, *EsGRAS45*, *EsGRAS47*, *EsGRAS48*, *EsGRAS56*, *EsGRAS62*, *EsGRAS66*, *EsGRAS68*, *EsGRAS74*, *EsGRAS76*, *EsGRAS83*, *EsGRAS95*, *EsGRAS102*, *EsGRAS108*, *EsGRAS113*, and *EsGRAS116*—likely resulted fromsegmental duplications (Fig. 3). These findings suggested that the expansion of *GRAS* gene family in *E. sibiricus* was predominantly driven by WGD, supplemented by localized segmental duplication. Furthermore, eight *GRAS* gene clusters were identified across chromosomes, which may explain the relatively high *GRAS* gene number observed in *E. sibiricus.* Cross-species collinearity analysis revealed that approximately 67.69% of *EsGRAS* genes exhibit orthologous relationships with *GRAS* genes in wheat (*T. aestivum*), whereas only 2.94% share orthology with those in *A. thaliana*. This sharp contrast highlighted that significant functional divergence has occurred between monocot and dicot *GRAS* gene lineages, possibly driven by distinct selection pressures and adaptive requirements.

In plants, the exon-intron structure of *GRAS* genes exhibits poor conservation, with exon numbers showing notable variation. In *E. sibiricus*, *EsGRAS* genes contain 1 to 9 exons (Fig. 2), a pattern comparable to that observed in other species such as *Hibiscus hamabo* (1–4 exons) [43], *Secale cereale* (1–6 exons) [44], and *Passiflora edulis* (1–4 exons) [45]. Interestingly, even among homologous gene pairs, exon number often differs substantially. For example, Es*GRAS109* possesses a single exon, whereas Es*GRAS97* contains 9. This discrepancies implied exon gain or loss events have occurred during evolution, contributing to structural variation. Despite the overall conservation of motif composition and arrangement among *EsGRAS* proteins (Fig. 2), a high degree of motif diversity was observed. Most *GRAS* proteins contains five canonical domains in the C-terminal region: LHR□, VHIID, LHR□, PFYRE, and SAW. The VHIID domain, which is central and contains highly conserved histidine and aspartic acid residues, is believed to play a critical role in protein–protein interactions and functional specificity. In some cases, non-polar residues such as leucine, isoleucine, and valine substitute for the conserved amino acids within this region, possibly due to neutral mutations that do not compromise the overall structure. Notably, some SCR subfamily memebers, such as *EsGRAS22*, *EsGRAS23*, and *EsGRAS47*, lack key residues in the VHIID domain, a feature also reported in *Raphanus sativus*[46], suggesting subfamily-specific structural divergence. These structural differences collectively indicated that the structural diversity among *EsGRAS* gene is likely correlated with their functional specialization.

Cis-element analysis identified 22 distinct types of regulatory elements associated with environmental stress response, hormone regulation, developmental processes, and light response (Fig. 5). Universally prevalent elements include ABRE, CAT-box, MRE, and GT1-motif [47]. Among these, ABRE and CAT-box are functionally linked to meristem development and hypoxic stress responses, whereas MRE and GT1-motif operate within light-responsive regulatory pathways [48]. Weits et al. [49] and Shukla et al. [50] demonstrated that apical meristem development during hypoxia is essential for initiating new leaf formation. Under such conditions, light serves as a signaling factor that activates stem cells via cytokinin (CK) signaling and associated metabolic processes[51]. The abundance of developmental elements (ABRE, CAT-box) in *GRAS* promoters suggests their involvement in plant hormones signalling [52, 53], particularly in response to GA, which influences plant height and morphology. Furthermore, key cis-acting regulatory elements (GT-1-motif, CAT–box, GATAT-motif) have been identified in *E. sibiricus GRAS* gene promoters [54]. Light-responsive elements such as the GT1-motif and MRE were also prevalent, reinforcing the notion that *GRAS* gene expression is tightly coordinated with photomorphogenic pathways. The enrichment of GA-responsive motifs, including the GARE and P-box, is consistent with the known involvement of *GRAS* genes—particularly those from the DELLA subfamily—in gibberellin signaling [55]. Additionally, binding motifs for other transcription factors (e.g., GTAC elements recognized by SPL proteins) were identified, suggesting complex transcriptional regulation [56]. Given the crucial role of *GRAS* genes in plant growth and development, future research should focus on functionally validating these cis-regulatory elements and exploring *GRAS* interactions to gain new insights into plant growth, morphology, and developmental processes.

Gene family members often possess conserved functional domains and structural features, enabling them to participate collaboratively in complex regulatory pathways and biological functions. Proteins within the same family frequently act in concert, much like batons in a relay race, forming intricate signaling cascades that control essential biological processes such as cell division, differentiation, organogenesis and apoptosis. In this context, protein-protein interaction (PPI) network analysis serves as a powerful tool to elucidate functional relationships among family members and their associated signaling partners, In the present study, key interaction nodes were identified within the GRAS protein network in *E. sibiricus*, including GID1, GA2OX, GA3OX, PAT1, PHYA, and NSP2. These components are centrally involved in gibberellin (GA) and light signaling pathways, as well as developmental and stress response networks. GID1 functions as a GA receptor, initiating DELLA protein degradation and thus activating GA-responsive gene expression. Its elevated expression during early panicle development and its coordinated regulation with the F-box protein GID2 and DELLA (e.g., OsSLR1) indicate a tightly regulated GA–DELLA signaling module involved in reproductive development and grain morphology. *GRAS* family members such as *GS6* and *SCL6-IIb*, which exhibit co-expression with GID1, have been implicated in the modulation of grain type and plant stature [56]. The GA oxidase genes, *GA2OX* and *GA3OX*, regulate GA homeostasis by controlling the biosynthesis and deactivation of bioactive GAs. Their manipulation has demonstrated profound phenotypic consequences. For example, overexpression of *GA2OX* in maize and rice results in dwarfism and increased tillering, while *AtGA2OX* overexpression delays *A. thaliana* flowering. *GA3OX2* mutants exhibit impaired flowering and sterility, whereas *GA3OX3* and *GA1OX1* mutants affect active GA levels and grain development [57, 58]. These findings underscore the significance of GA metabolic regulation in shaping plant architecture and reproductive success. Photoreceptor-related components such as PAT1 and PHYA also occupy central positions in the PPI network. PAT1 mediates far-red light signaling, influencing photomorphogenesis and developmental transitions, including axillary bud formation and floral induction [59]. PHYA PHYA demonstrates light quality–dependent expression, with studies in tea (*Camellia sinensis*) showing that specific wavelengths (e.g., purple or red light)markedly alter PHYA and PHYB expression profiles, thereby impacting photosynthetic and circadian regulation [60]. NSP2, a *GRAS* family transcriptional regulator, governs the symbiotic signaling by regulating genes associated with symbiotic and strigolactone biosynthesis and root nodule formation Its role extends beyond legumes, impacting arbuscular mycorrhizal fungal symbiosis and nutrient uptake in diverse plant species [61]. Additional *GRAS* network components such as SOC1 and MOC1 are also functionally relevant. MOC1, primarily expressed in axillary meristems, is indisoesable for axillary bud initiation and outgrowth. *moc1* mutants display a phenotype lacking tillers and a solitary main stem, highlighting its role in shoot branching [62]. SOC1 facilitates flowering by upregulating key floral meristem genes such as *LEAFY (LFY)* and *APETALA1 (AP1)* and forms a dimer with FUL to activate LFY expression, further regulating floral organogenesis and meristem determinacy [63]. Identifying these critical hub proteins is essential for elucidating cellular signaling pathways and central metabolic regulation. Collectively, these results suggest that the *GRAS* protein family interacts extensively with multiple hormone and environmental signaling pathways. The identification of hub proteins such as GID1, GA2OX, PAT1, and NSP2 advances our understanding of the *GRAS* interactome and provides a mechanistic framework for the regulation of key developmental and adaptive processes in *E. sibiricus*.

In living organisms, gene expression precedes and is essential for gene function, with expression patterns intricately linked to gene roles [22]. The *GRAS* gene family is widely involved in plant growth and development, playing a key regulatory roles across various developmental stages—from seedlings to maturity [1, 32]. In kiwifruit, genes such as *AcGRAS6* and *AcGRAS21* are upregulated under salt stress. These genes, involved in metabolic and biosynthetic processes, enhance salt tolerance by positively modulating salt stress responses and mitigating salt-induced damage [64]. Under drought stress, *GRAS* genes can strengthen plant drought resistance by maintaining ion homeostasis. For instance, In soybean, overexpression of *GmFER1* enhances drought adaptability by upregulating the Na^+ transporter *GmSOS1*, thereby promoting Na^+ efflux and increasing intracellular K^+ and Ca^{2+} levels to stabilize ion balance [65]. In *Hibiscus hamabo*, *HhGRAS14* expression is significantly upregulated by drought, salt stress, and ABA treatment. Silencing *HhGRAS14* reduces drought and salt tolerance, whereas its overexpression in *A. thaliana* enhances tolerance and decreases ABA sensitivity, underscoring its integrative role in ABA signaling in stress responses [43]. NGR5, a key component in gibberellin signaling pathway, interacts with the GA receptor GID1. GA promotes NGR5 degradation, leading to reduced H3K27me3 epigenetic modifications and activation of downstream target genes, thereby inhibiting rice tillering [66]. Overall, *GRAS* genes are crucial player in plant responses to abiotic stresses. This study demonstrates that *EsGRAS128* was continuously upregulated under salt stress, suggesting a potential role as a key negative regulator. This makes *EsGRAS128* a promising target for future exploration in salt stress adaptation and genetic improvement strategies. Similarly, in rice, *OsGRAS10* is upregulated under salt stress and may contribute to early-stage salt stress response by regulating ion homeostasis and antioxidant defense systems [67]. In maize, the heterologous expression of *ZmGRAS72* in *A. thaliana* significantly enhances drought and salt stress tolerance, increases chlorophyll content, reduces malondialdehyde levels, and boosts peroxidase activity [68]. In this study, *EsGRAS90* and *EsGRAS95* were significantly upregulated under drought stress. In wheat, six *TaGRAS* genes -*TaGRAS8*, *TaGRAS27*, *TaGRAS53*, *TaGRAS54*, *TaGRAS98*, and *TaGRAS122*)- showed 10-fold induction under drought indicating potential roles in enhancing drought resistance by regulating related physiological processes [69]. Notablly, *EsGRAS95* was also upregulated under ABA treatment, mirroring its drought-induced xpression pattern and suggesting a possible role in ABA-mediated stress responses. In eucalyptus, 18 *GRAS* genes showed differential expression under ABA and GA3 treatment, with 11 upregulated. Among them, *EgrGRAS68*, *EgrGRAS34*, and *EgrGRAS13* showed more than four-fold increases compared to controls, indicating they may be involved in ABA signaling and drought resistance [70]. In tomato, *SlGRAS4* enhances drought tolerance by directly regulating the ABA signaling gene *SlSnRK2.4* [71]. Similarly, in *H. hamabo*, *HhGRAS14* mediates drought and salt tolerance through ABA signaling integration [43]. Under GA treatment, *EsGRAS113* was significantly up-regulated. As a member of the DELLA subfamily, this observation is consistent with previously reported roles of DELLA proteins in GA signal transduction, plant growth, and stress adaptation [72]. In *A. thaliana*, DELLA subfamily members (e.g., GAI, RGA, RGL1,RGL2) act as negative regulators of GA negatively regulate GA signaling. They restrict plant growth by inhibiting GA signals, a process reversed by GA-induced degradation of DELLA proteins. For instance, RGA and GAI inhibit stem elongation and leaf expansion, while *RGL1/RGL2* affect seed germination in *A. thaliana* [73]. Based on these fondings, we propose that the *GRAS* gene family plays a crucial role in abiotic stress resistance in *E. sibiricus*. Specifically, *EsGRAS128, EsGRAS90, EsGRAS95*, and *EsGRAS113* may function as key mediators of stress responses.

5. conclusion

This study represents the first genome-wide investigation of the *GRAS* gene family in *E. sibiricus*, identifying 130 *EsGRAS* members primarily expanded through segmental duplications. Bioinformatic analyses revealed fundamental genetic characteristics, including conserved protein sequences and

structures, hormone/stress-responsive cis-elements in *EsGRAS* promoters, and regulatory interactions through protein-protein networks with phytohormone regulators (GID1, GA2OX, GA3OX), light sensors (PAT1, PHYA), and symbiosis factor NSP2. Expression profiling under four abiotic stresses demonstrated significant induction of *EsGRAS90*, *EsGRAS95*, *EsGRAS128*, and *EsGRAS113*. Collectively, this study elucidates the genetic evolution and biological functions of *EsGRAS* genes, establishing a foundation for future functional characterization and stress-adaptation applications.

Abbreviations

GRAS GAI RGA SCR

GAI Gibberellic Acid Insensitivity

RGA Repressor of GA1-3 mutant

SCR Scarecrow

MW Molecular weight

PI isoelectric point

ABA abscisic acid

GA gibberellin

Declarations

Ethics approval and consent to participate

This article does not contain any studies involving human participants or animals performed by the authors. These methods were carried out by relevant guidelines and regulations. *E. sibiricus* used in this study is a prevalent wild species in the Qinghai area. Based on international standards, all the experimental research and field studies on plants, including the collection of plant material were approved by Institute of Animal Sciences. These materials are stored in Institute of Animal Sciences of Chinese Academy of Agricultural Sciences.

Consent for publication

Not applicable.

Availability of data and materials

The genome sequences of *A. thaliana, O. sativa, B. distachyon, and T. aestivum* were downloaded from phytozome database (https://phytozome-next.jgi.doe.gov/). The datasets supporting the results of this article are included in the article and Additional files.

Funding

This work was supported by the National Key Research and Development Program of China (2023YFD1200303), the earmarked fund for China Agriculture Research System (CARS-34), the Aricultural Germplasm Conservation Services (22250241), the Key Research and Development Pro gram of the Xinjiang Uygur Autonomous Region (2023B02031), and the Xinjiang Graduate Student Scientific Research Innovation Program (XJ2025G108).

Authors' contributions

performed the experiments with the help of D.Y., L.M., X.M., J.T., X.M., K.X., and W.L. analyzed the sequencing data; X.W., J.T., D.Y., Z.J., W.L., M.H., and W.L. designed the experiments, interpreted the results, and wrote the manuscript. All authors read and approved of the final manuscript.

Acknowledgements

We thank all our colleagues for providing useful discussions and technical assistance. We are very grateful to the editor and reviewers for critically evaluating the manuscript and providing constructive comments for its improvement.

Competing Interests

The authors declare that they have no conflict of interest.

References

1. Lin J, Wu J, Zhang D, Cai X, Du L, Lu L, Liu C, Chen S, Yao Q, Xie S, Xu X, Wang X, Liu R, Qin Y, Zheng P. The *GRAS* gene family and its roles in pineapple (*Ananas comosus* L.) developmental regulation and cold tolerance. *BMC Plant Biol.* 2024;24(1):1204.
2. Bolle C. The role of *GRAS* proteins in plant signal transduction and development. *Planta.* 2004;218(5):683-92.

3. Jaiswal V, Kakkar M, Kumari P, Zinta G, Gahlaut V, Kumar S. Multifaceted roles of *GRAS* transcription factors in growth and stress responses in plants. *iScience*. 2022;25(9):105026.
4. Sun X, Xue B, Jones WT, Rikkerink E, Dunker AK, Uversky VN. A functionally required unfoldome from the plant kingdom: intrinsically disordered N-terminal domains of GRAS proteins are involved in molecular recognition during plant development. *Plant Mol Biol.* 2011;77(3):205-23.
5. Zhang X, Yang X, He Q, Wang Y, Liang G, Liu T: Genome-wide identification and characterization of the *GRAS* transcription factors in garlic (*Allium sativum* L.). *Front Plant Sci.* 2022;13:890052.
6. Kumari P, Gahlaut V, Kaur E, Singh S, Kumar S, Jaiswal V: Genome-wide identification of *GRAS* transcription factors and their potential roles in growth and development of rose (*Rosa chinensis*). *Journal of Plant Growth Regulation.* 2023, 42(3):1505-1521.
7. Ishikawa M, Fujiwara A, Kosetsu K, Horiuchi Y, Kamamoto N, Umakawa N, Tamada Y, Zhang L, Matsushita K, Palfalvi G, Nishiyama T, Kitasaki S, Masuda Y, Shiroza Y, Kitagawa M, Nakamura T, Cui H, Hiwatashi Y, Kabeya Y, Shigenobu S, Aoyama T, Kato K, Murata T, Fujimoto K, Benfey PN, Hasebe M, Kofuji R: *GRAS* transcription factors regulate cell division planes in moss overriding the default rule. *Proceedings of the National Academy of Sciences of the United States of America.* 2023; 120(4):e2210632120.
8. Wang X, Dong X, Li P, Li M, Wang Z, Zhou Q, Liu Z, Yan L: Genome-wide identification of the *GRAS* transcription factor family in *Medicago ruthenica* and expression analysis under drought stress. *Agronomy.* 2025, 15(2):306.
9. Neves C, Ribeiro B, Amaro R, Expósito J, Grimplet J, Fortes AM: Network of *GRAS* transcription factors in plant development, fruit ripening and stress responses. *Hortic Res.* 2023, 10(12):uhad220.
10. Niu Y, Zhao T, Xu X, Li J: Genome-wide identification and characterization of *GRAS* transcription factors in tomato (*Solanum lycopersicum*). *PeerJ.* 2017, 5:e3955.
11. Wang Z, Wong DCJ, Wang Y, Xu G, Ren C, Liu Y, Kuang Y, Fan P, Li S, Xin H, Liang Z: GRAS-domain transcription factor PAT1 regulates jasmonic acid biosynthesis in grape cold stress response. *Plant Physiol0.* 2021, 186(3):1660-1678.
12. Zhang H, Mi L, Xu L, Yu C, Li C, Chen C: Genome-wide identification, characterization, interaction network and expression profile of *GRAS* gene family in sweet orange (*Citrus sinensis*). *Sci Rep.* 2019, 9(1):2156.
13. Avilés-Cárdenas JD, Molinero-Rosales N, Pérez-Tienda J, Rosas-Díaz T, Castillo AG, García-Garrido JM: Enhancing arbuscular mycorrhiza symbiosis effectiveness through the involvement of the tomato *GRAS* transcription factor *SCL3/SlGRAS18. Plant physiology and biochemistry.* 2024, 215:109019.
14. Liu T, Liu Z, Fan J, Yuan Y, Liu H, Xian W, Xiang S, Yang X, Liu Y, Liu S, Zhang M, Jiao Y, Cheng S, Doyle JJ, Xie F, Li J, Tian Z: Loss of Lateral suppressor gene is associated with evolution of root nodule symbiosis in *Leguminosae*. *Genome Biol.* 2024, 25(1):250.
15. Shah SH, Carlson JE, Niklas KJ, Benavides-Mendoza A, Ricachenevsky FK: Editorial: Deciphering mechanisms of plant adaptation and resistance under cold temperature stress. *Front Plant Sci.* 2024, 15:1460573.
16. He Z, Tian Z, Zhang Q, Wang Z, Huang R, Xu X, Wang Y, Ji X: Genome-wide identification, expression and salt stress tolerance analysis of the *GRAS* transcription factor family in *Betula platyphylla*. *Front Plant Sci.* 2022, 13:1022076.
17. Hirano K, Asano K, Tsuji H, Kawamura M, Mori H, Kitano H, Ueguchi-Tanaka M, Matsuoka M: Characterization of the molecular mechanism underlying gibberellin perception complex formation in rice. *Plant Cell.* 2010, 22(8):2680-2696.
18. Ma HS, Liang D, Shuai P, Xia XL, Yin WL: The salt- and drought-inducible poplar *GRAS* protein SCL7 confers salt and drought tolerance in *Arabidopsis thaliana*. *J Exp Bot.* 2010, 61(14):4011-4019.
19. Xu W, Chen Z, Ahmed N, Han B, Cui Q, Liu A: Genome-wide identification, evolutionary analysis, and stress responses of the *GRAS* Gene family in castor beans. *Int J Mol Sci.* 2016, 17(7):1004.
20. Heo JO, Chang KS, Kim IA, Lee MH, Lee SA, Song SK, Lee MM, Lim J: Funneling of gibberellin signaling by the *GRAS* transcription regulator scarecrow-like 3 in the *Arabidopsis* root. *Proc Natl Acad Sci U S A.* 2011, 108(5):2166-2171.
21. Liu Y, Huang W, Xian Z, Hu N, Lin D, Ren H, Chen J, Su D, Li Z: Overexpression of *SlGRAS40* in tomato enhances tolerance to abiotic stresses and influences auxin and gibberellin signaling. *Front Plant Sci.* 2017, 8:1659.
22. Weng Y, Chen X, Hao Z, Lu L, Wu X, Zhang J, Wu J, Shi J, Chen J: Genome-wide analysis of the *GRAS* gene family in *Liriodendron chinense* reveals the putative function in abiotic stress and plant development. *Front Plant Sci.* 2023, 14:1211853.
23. Wang Q, Guo C, Li Z, Sun J, Deng Z, Wen L, Li X, Guo Y: Potato NAC transcription factor *StNAC053* enhances salt and drought tolerance in transgenic *Arabidopsis*. *Int J Mol Sci* 2021, 22(5):2568.
24. Liao Z, Zhang Y, Yu Q, Fang W, Chen M, Li T, Liu Y, Liu Z, Chen L, Yu S, Xia H, Xue HW, Yu H, Luo L: Coordination of growth and drought responses by GA-ABA signaling in rice. *New Phytol.* 2023, 240(3):1149-1161.
25. Chen J, Yan Q, Li J, Feng L, Zhang Y, Xu J, Xia R, Zeng Z, Liu Y: The *GRAS* gene family and its roles in seed development in litchi (*Litchi chinensis* Sonn). *BMC Plant Biol* 2021, 21(1):423.
26. Guo P, Wen J, Yang J, Ke Y, Wang M, Liu M, Ran F, Wu Y, Li P, Li J, Du H: Genome-wide survey and expression analyses of the *GRAS* gene family in *Brassica napus* reveals their roles in root development and stress response. *Planta.* 2019, 250(4):1051-1072.
27. Sun X-L, Li Y, Cai H, Bai X, Ji W, Ji Z-J, Zhu Y-M: *Arabidopsis* bZIP1 transcription factor binding to ABRE cis-element regulates abscisic acid signal transduction. *Acta Agronomica Sinica.* 2011, 37(4):612-619.
28. Zheng Y, Wang N, Zhang Z, Liu W, Xie W: Identification of flowering regulatory networks and hub genes expressed in the leaves of *Elymus sibiricus* L. using comparative transcriptome analysis. *Front Plant Sci.* 2022, 13:877908.
29. De Y, Yan W, Gao F, Mu H: Unraveling the signaling pathways of phytohormones underlying salt tolerance in *Elymus sibiricus*: A transcriptomic and metabolomic approach. *Genomics.* 2024, 116(5):110893.

30. Yan J, Li X, Wang L, Li D, Ji C, Yang Z, Chen L, Zhang C, You M, Yan L, Gou W, Lei X, Ji X, Li Y, Wu Q, Mao D, Chang D, Jia S, Li P, Zhang J, Xiong Y, Xiong Y, Han M, Chen Z, Cheng X, Tang J, Xie W, Liu W, Zheng H, Ma X, Yan X, Bai S: A high-continuity and annotated reference genome of allotetraploid Siberian wildrye (*Elymus sibiricus* L., Poaceae: Triticeae). *In bioRxiv.* 2024.2004.2017.589894.
31. Shen WJ, Liu B, Guo JL, Yang Y, Li XH, Chen J, Dou QW: Chromosome-scale assembly of the wild cereal relative *Elymus sibiricus*. *Scientific Data.* 2024, 11(1):823.
32. Xie Z, Yang D, Zhou Z, Li K, Yi P, Liu A, Zhou Z, Tu X: A genome-wide analysis of the *GRAS* gene family in upland cotton and a functional study of the role of the *GhGRAS55* gene in regulating early maturity in cotton. *Biotechnol J.* 2023, 18(12):e2300201.
33. Chen C, Chen H, Zhang Y, Thomas HR, Frank MH, He Y, Xia R: TBtools: An integrative toolkit developed for interactive analyses of big biological data. *Mol Plant.* 2020, 13(8):1194-1202.
34. Lescot M, Déhais P, Thijs G, Marchal K, Moreau Y, Van de Peer Y, Rouzé P, Rombauts S: PlantCARE, a database of plant cis-acting regulatory elements and a portal to tools for in silico analysis of promoter sequences. *Nucleic Acids Res.* 2002, 30(1):325-327.
35. Zhang C, Liu S, Liu D, Guo F, Yang Y, Dong T, Zhang Y, Ma C, Tang Z, Li F *et al*: Genome-wide survey and expression analysis of *GRAS* transcription factor family in sweetpotato provides insights into their potential roles in stress response. *BMC Plant Biol.* 2022, 22(1):232.
36. Sun Y, Yuan T: Genome-wide analysis of *GRAS* gene family and functional identification of a putative development and maintenance of axillary meristematic tissue gene *PlGRAS22* in *Paeonia ludlowii. Int J Biol Macromol.* 2025, 297:139879.
37. Niu X, Chen S, Li J, Liu Y, Ji W, Li H: Genome-wide identification of *GRAS* genes in *Brachypodium distachyon* and functional characterization of *BdSLR1* and *BdSLRL1*. *BMC Genomics.* 2019, 20(1):635.
38. Wang S, Duan Z, Yan Q, Wu F, Zhou P, Zhang J: Genome-wide identification of the *GRAS* family genes in melilotus albus and expression analysis under various tissues and abiotic stresses. *Int J Mol Sci.* 2022, 23(13):7403.
39. Dong X, Deng H, Ma W, Zhou Q, Liu Z: Genome-wide identification of the MADS-box transcription factor family in autotetraploid cultivated alfalfa (*Medicago sativa* L.) and expression analysis under abiotic stress. *BMC Genomics.* 2021, 22(1):603.
40. To VT, Shi Q, Zhang Y, Shi J, Shen C, Zhang D, Cai W: Genome-wide analysis of the *GRAS* gene family in barley (*Hordeum vulgare* L.). *Genes (Basel).* 2020, 11(5).
41. Tong N, Li D, Zhang S, Tang M, Chen Y, Zhang Z, Huang Y, Lin Y, Cheng Z, Lai Z: Genome-wide identification and expression analysis of the *GRAS* family under low-temperature stress in bananas. *Front Plant Sci.* 2023, 14:1216070.
42. Kong H, Landherr LL, Frohlich MW, Leebens-Mack J, Ma H, dePamphilis CW: Patterns of gene duplication in the plant *SKP1* gene family in angiosperms: evidence for multiple mechanisms of rapid gene birth. *Plant J.* 2007, 50(5):873-885.
43. Ni L, Wang Z, Liu X, Wu S, Hua J, Liu L, Yin Y, Li H, Gu C: Genome-wide study of the *GRAS* gene family in *Hibiscus hamabo* Sieb. et Zucc and analysis of *HhGRAS14*-induced drought and salt stress tolerance in *Arabidopsis*. *Plant Sci.* 2022, 319:111260.
44. Fan Y, Wan X, Zhang X, Zhang J, Zheng C, Yang Q, Yang L, Li X, Feng L, Zou L, Xiang D: *GRAS* gene family in rye (*Secale cereale* L.): genome-wide identification, phylogeny, evolutionary expansion and expression analyses. *BMC Plant Biol.* 2024, 24(1):46.
45. Cai X, Li D, Liu C, Chen J, Wei X, Hu S, Lu L, Chen S, Yao Q, Xie S *et al*: Identification and characterization of *GRAS* genes in passion fruit (*Passiflora edulis* Sims) revealed their roles in development regulation and stress response. *Plant Cell Reports.* 2025, 44(2):46.
46. Li C, Wang K, Chen S, Zhang X, Zhang X, Fan L, Dong J, Xu L, Wang Y, Li Y, Liu L: Genome-wide identification of *RsGRAS* gene family reveals positive role of *RsSHRc* gene in chilling stress response in radish (*Raphanus sativus* L.). *Plant Physiol Biochem.* 2022, 192:285-297.
47. Hernandez-Garcia CM, Finer JJ: Identification and validation of promoters and cis-acting regulatory elements. *Plant Sci.* 2014, 217:109-119.
48. Ibraheem O, Botha CE, Bradley G: In silico analysis of cis-acting regulatory elements in 5' regulatory regions of sucrose transporter gene families in rice (*Oryza sativa* Japonica) and *Arabidopsis thaliana*. *Comput Biol Chem.* 2010, 34(5-6):268-283.
49. Weits DA, Kunkowska AB, Kamps NCW, Portz KMS, Packbier NK, Nemec Venza Z, Gaillochet C, Lohmann JU, Pedersen O, van Dongen JT, Licausi F: An apical hypoxic niche sets the pace of shoot meristem activity. *Nature.* 2019, 569(7758):714-717.
50. Shukla V, Lombardi L, Iacopino S, Pencik A, Novak O, Perata P, Giuntoli B, Licausi F: Endogenous hypoxia in lateral root primordia controls root architecture by antagonizing auxin signaling in *Arabidopsis*. *Molecular Plant.* 2019, 12(4):538-551.
51. Pfeiffer A, Janocha D, Dong Y, Medzihradszky A, Schöne S, Daum G, Suzaki T, Forner J, Langenecker T, Rempel E, Schmid M, Wirtz M, Hell R, Lohmann JU: Integration of light and metabolic signals for stem cell activation at the shoot apical meristem. *ELife.* 2016, 5:e17023.
52. İlhan E, Büyük İ, İnal B: Transcriptome - Scale characterization of salt responsive bean *TCP* transcription factors. *Gene.* 2018, 642:64-73.
53. Rouster J, Leah R, Mundy J, Cameron-Mills V: Identification of a methyl jasmonate-responsive region in the promoter of a lipoxygenase 1 gene expressed in barley grain. *Plant J.* 1997, 11(3):513-523.
54. Zhu T, Liu Y, Ma L, Wang X, Zhang D, Han Y, Ding Q, Ma L: Genome-wide identification, phylogeny and expression analysis of the *SPL* gene family in wheat. *BMC Plant Biol.* 2020, 20(1):420.
55. Wang Y-X, Liu Z-W, Wu Z-J, Li H, Wang W-L, Cui X, Zhuang J: Genome-wide identification and expression analysis of *GRAS* family transcription factors in tea plant (*Camellia sinensis*). *Sci Rep* 2018, 8(1):3949.
56. Chen S, Li F, Ouyang W, Chen S, Luo S, Liu J, Li G, Lin Z, Liu YG, Xie X: Time-course transcriptome and chromatin accessibility analyses reveal the dynamic transcriptional regulation shaping spikelet hull size. *Plant J.* 2025, 122(1):e70141.
57. Sun J, Zhang X, Feng J, Ma X, Ji Y, Chen S, Li J, Li D, Wang X, Zhao L: The transcription factor *GmFULc* regulates soybean plant height by binding the promoter of a gibberellin-responsive gene. *Plant Physiol.* 2025, 197(2):kiaf021.

58. Phillips AL, Huttly AK, Alarcón-Reverte R, Clark SJ, Jaworek P, Tarkowská D, Sokolowska P, Steele D, Riche A, Hawkesford MJ, Thomas SG, Hedden P, Pearce S: GIBBERELLIN 3-OXIDASE genes regulate height and grain size in bread wheat. *J Exp Bot.* 2025,10:eraf151.
59. Muntha ST, Zhang L, Zhou Y, Zhao X, Hu Z, Yang J, Zhang M: Phytochrome A signal transduction 1 and CONSTANS-LIKE 13 coordinately orchestrate shoot branching and flowering in leafy Brassica juncea. *Plant Biotechnol J.* 2019, 17(7):1333-1343.
60. Sineshchekov V, Koppel L: Phytochrome A in plants comprises two structurally and functionally distinct populations—water-soluble phyA' and amphiphilic phyA". *Biophys Rev.* 2022, 14(4):905-921.
61. Kun Y, Zhang H, Yu C, Luo N, Yan J, Zheng S, Hu Q, Zhang D, Kou L, Meng X, Jing Y, Chen M, Ban X, Yan Z, Lu Z, Wu J, Zhao Y, Liang Y, Wang Y, Xiong G, Chu J, Wang E, Li J, Wang B: Low phosphorus promotes NSP1–NSP2 heterodimerization to enhance strigolactone biosynthesis and regulate shoot and root architecture in rice. *Mol Plant.* 2023, 16(11):1811-1831.
62. Li X, Qian Q, Fu Z, Wang Y, Xiong G, Zeng D, Wang X, Liu X, Teng S, Hiroshi F, Yuan M, Luo D, Han B, Li J: Control of tillering in rice. *Nature.* 2003, 422(6932):618-621.
63. Xu X, Tao J, Xing A, Wu Z, Xu Y, Sun Y, Zhu J, Dai X, Wang Y: Transcriptome analysis reveals the roles of phytohormone signaling in tea plant (*Camellia sinensis* L.) flower development. *BMC Plant Biol.* 2022, 22(1):471.
64. Zhu L, Yin T, Zhang M, Yang X, Wu J, Cai H, Yang N, Li X, Wen K, Chen D, Zhang H, Liu X: Genome-wide identification and expression pattern analysis of the kiwifruit *GRAS* transcription factor family in response to salt stress. *BMC Genomics.* 2024, 25(1):12.
65. Wang L, Ding X, Gao Y, Yang S: Genome-wide identification and characterization of GRAS genes in soybean (Glycine max). *BMC Plant Biol* 2020, 20(1):415.
66. Wu K, Wang S, Song W, Zhang J, Wang Y, Liu Q, Yu J, Ye Y, Li S, Chen J, Zhao Y, Wang J, Wu X, Wang M, Zhang Y, Liu B, Wu Y, Harberd NP, Fu X: Enhanced sustainable green revolution yield via nitrogen-responsive chromatin modulation in rice. *Science.* 2020, 367(6478):eaaz2046.
67. Lee C, Chung C-T, Hong W-J, Lee Y-S, Lee J-H, Koh H-J, Jung K-H: Transcriptional changes in the developing rice seeds under salt stress suggest targets for manipulating seed quality. *Front Plant Sci.* 2021, 12:748273.
68. She M, Zheng D, Zhang S, Ke Z, Wu Z, Zou H, Zhang Z: Functional analysis of maize *GRAS* transcription factor gene *ZmGRAS72* in response to drought and salt stresses. *Agric Commun.* 2024, 2(3):100054.
69. Guan Y, Wang K, Zhao J, Miao X, Li X, Song P, Hu H, Zhang S, Li C: Genome-wide identification of *TaeGRASs* responsive to biotic stresses and functional analysis of *TaeSCL6* in wheat resistance to powdery mildew. *BMC Genomics.* 2024, 25(1):1149.
70. Lu H, Xu J, Li G, Zhong T, Chen D, Lv J: Genome-wide identification and expression analysis of *GRAS* gene family in Eucalyptus grandis. *BMC Plant Biol.* 2024, 24(1):573.
71. Liu Y, Wen L, Shi Y, Su D, Lu W, Cheng Y, Li Z: Stress-responsive tomato gene *SlGRAS4* function in drought stress and abscisic acid signaling. *Plant sci.* 2021, 304:110804.
72. Yu S, Galvão VC, Zhang YC, Horrer D, Zhang TQ, Hao YH, Feng YQ, Wang S, Schmid M, Wang JW: Gibberellin regulates the *Arabidopsis* floral transition through miR156-targeted SQUAMOSA promoter binding-like transcription factors. *Plant Cell.* 2012, 24(8):3320-3332.
73. Khan Y, Xiong Z, Zhang H, Liu S, Yaseen T, Hui T: Expression and roles of *GRAS* gene family in plant growth, signal transduction, biotic and abiotic stress resistance and symbiosis formation-a review. *Plant biol (Stuttg).* 2022, 24(3):404-416.

Figures

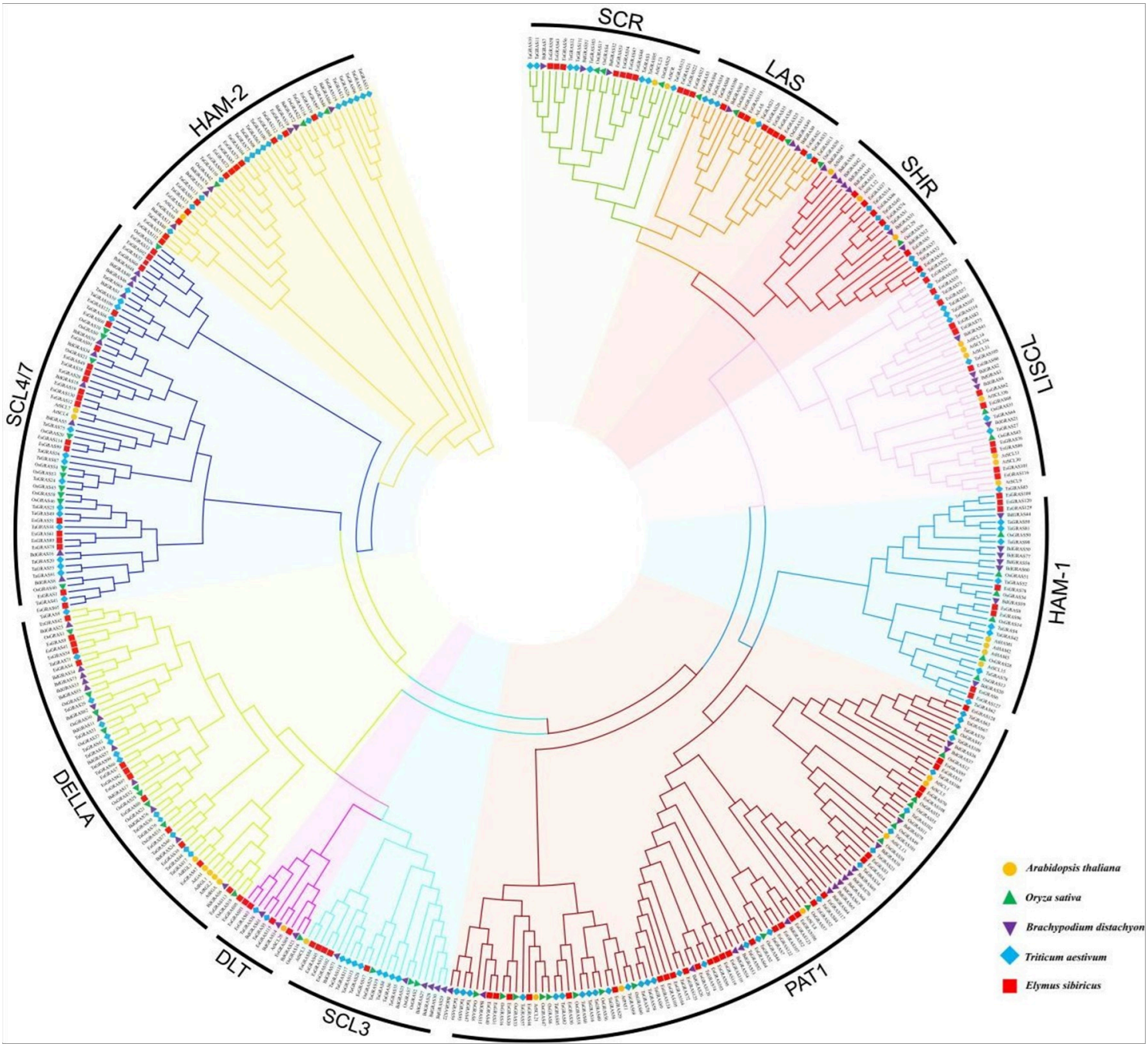

Figure 1

Evolutionary analysis of the *GRAS* candidate genes in *E.sibiricus.*

Figure 2

Detailed information on the conserved motifs, functional domains, and exon-intron organization of *GRAS* candidate genes in *E.sibiricus*where (A) represents conserved motifs, (B) represents functional domains, and (C) represents exon-intron organization.

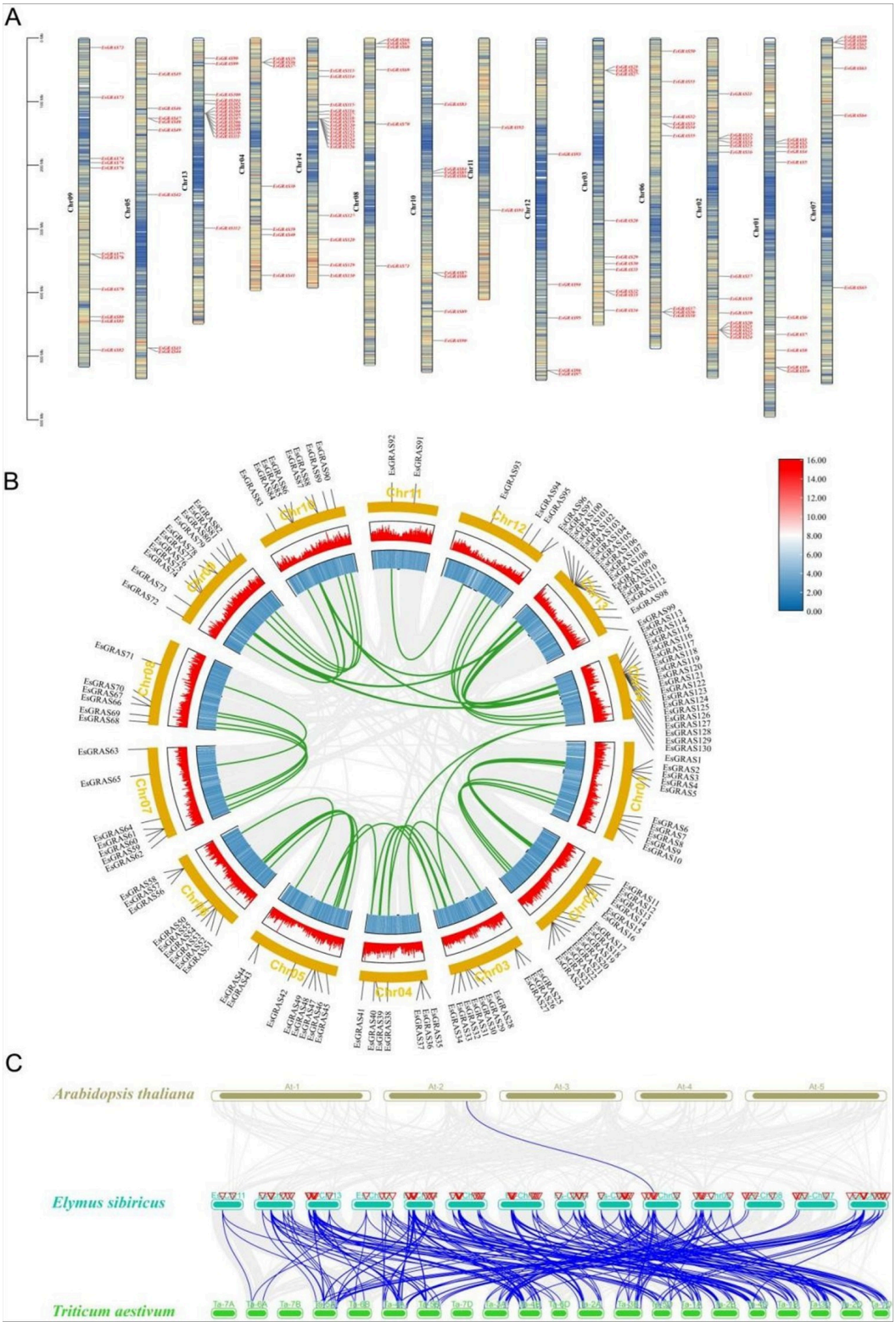

Figure 3

Chromosomal distribution and synteny analysis of *GRAS* candidate genes in *E.sibiricus*. (A) Spatial distribution of *GRAS* candidate genes on the chromosomes of *E.sibiricus*. (B) Intra-species synteny analysis describing the chromosomal localization of *GRAS*candidate genes. (C) Inter-species synteny analysis illustrating the relationship of *GRAS* candidate genes among *A. thaliana*, *E.sibiricus*and wheat. Colored lines represent the syntenic relationships of *GRAS*candidate genes between *E.sibiricus* and other plant species.

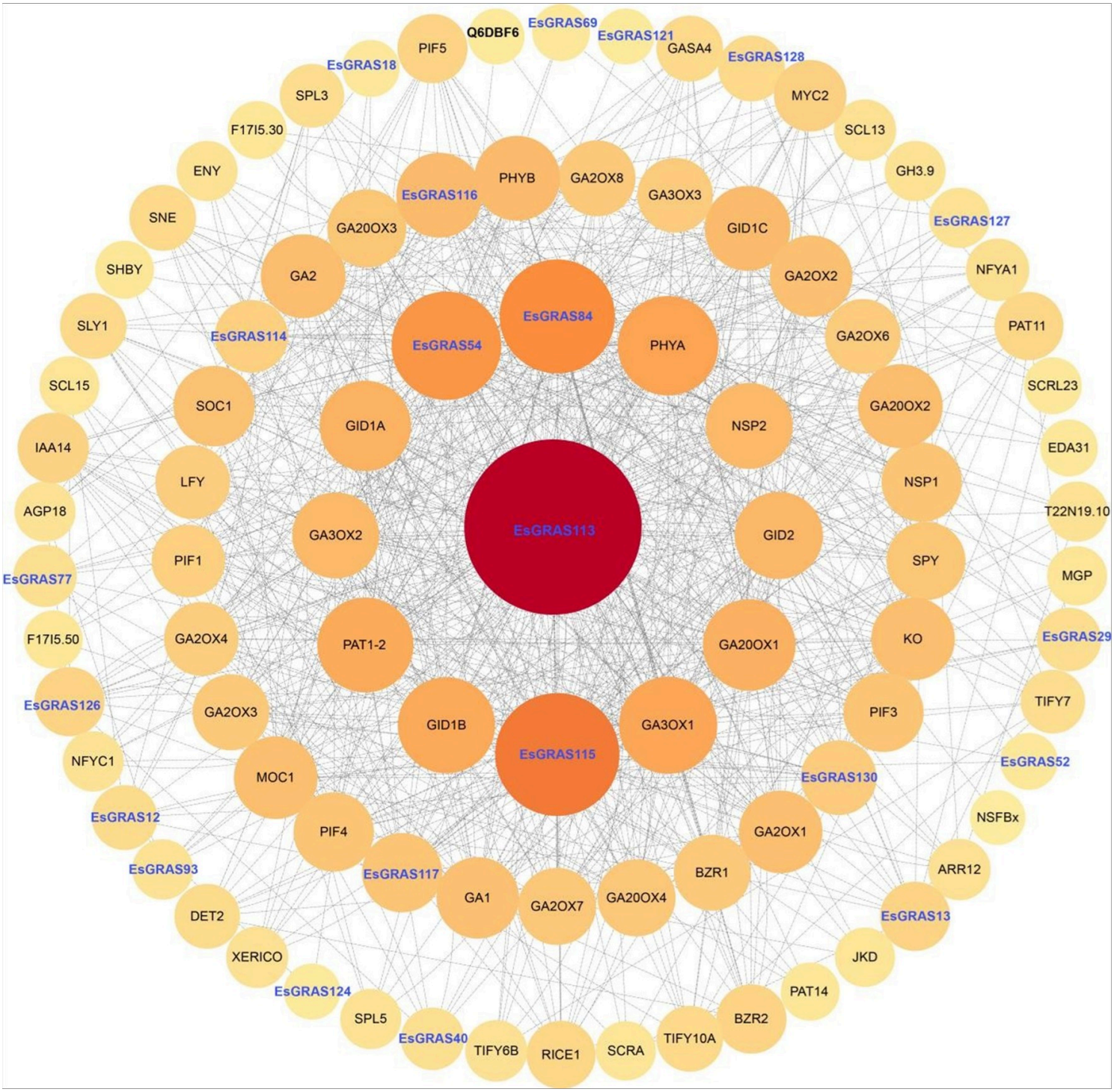

Figure 4

Predicted regulatory network of *GRAS* and its interacting proteins. Sky blue lines represent data from selected databases; purple lines are experimentally validated interactions; dark blue lines indicate gene co-occurrence; green lines represent text mining results; black lines denote co-expression; light blue lines indicate protein homology.

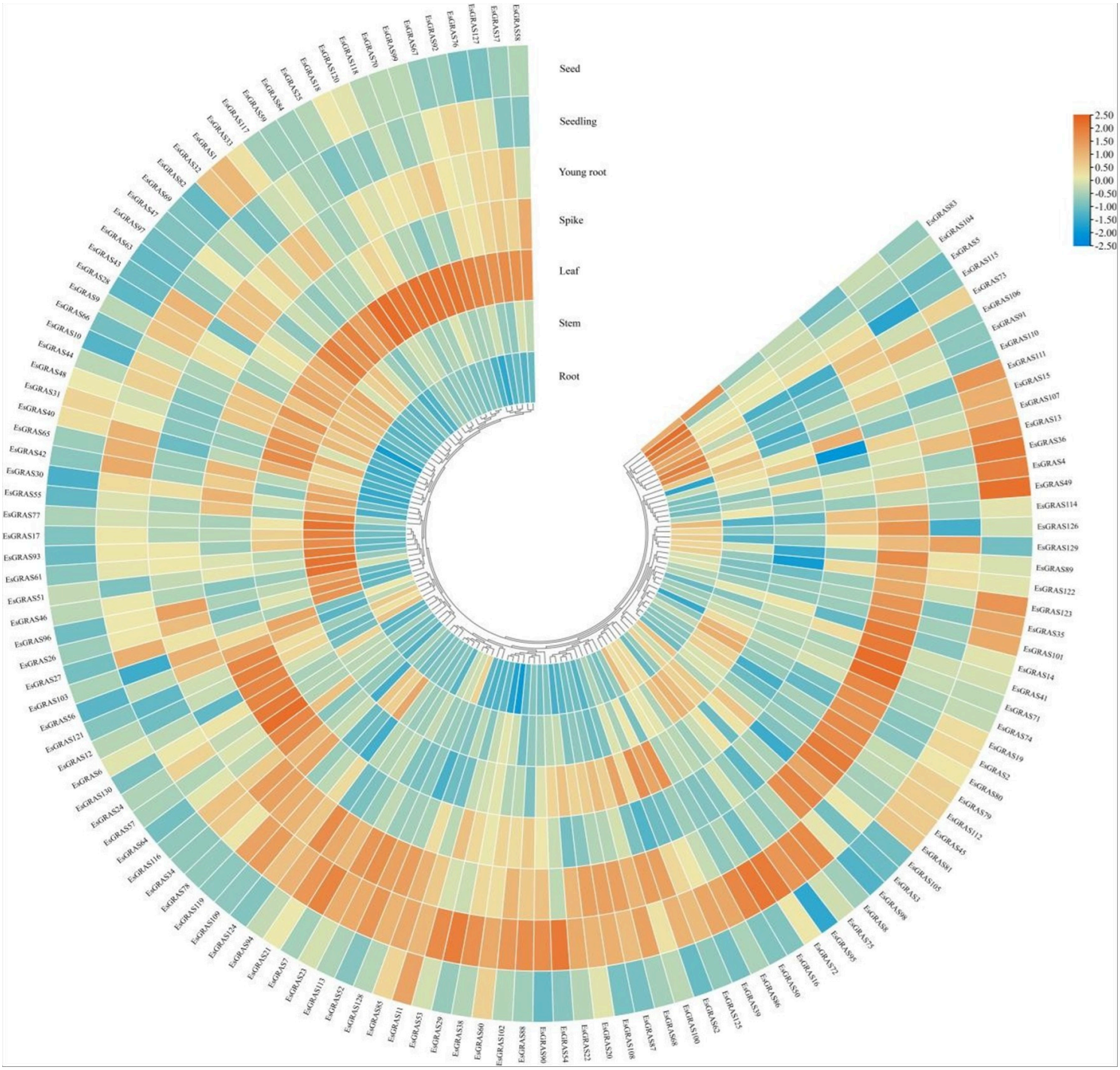

Figure 5

Quantitative analysis of the number of cis-acting regulatory elements in *GRAS* candidate genes. Different color shades and corresponding grid numbers represent the number of distinct promoter elements identified in the *GRAS* candidate genes. The multicolored histogram shows the total number of cis-acting regulatory elements in each functional category: blue represents environment stress-related elements, orange represents hormone response elements, yellow represents growth and development-related elements, and green represents light response elements.

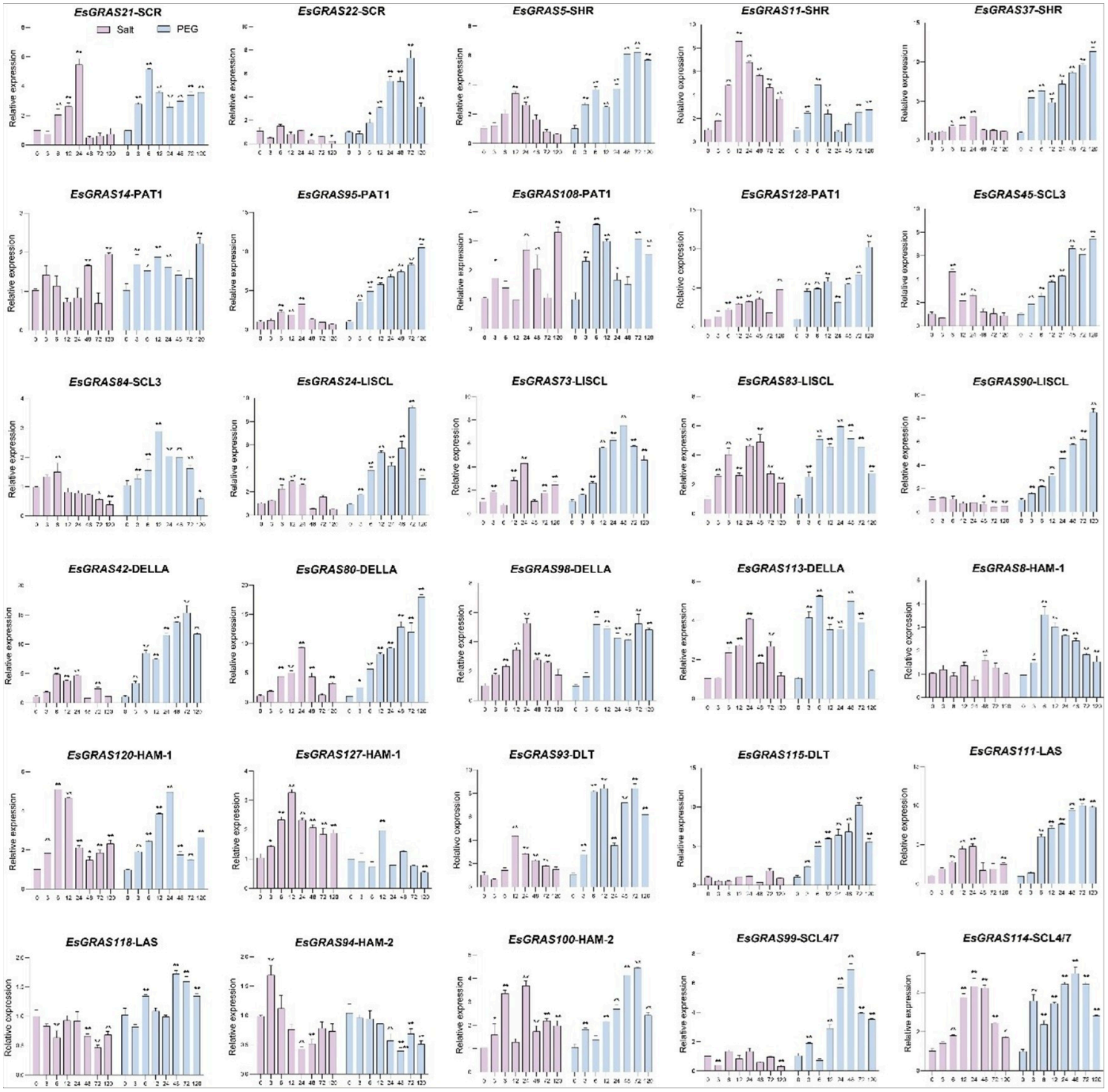

Figure 6

Expression levels of *GRAS* candidate genes in different tissues.

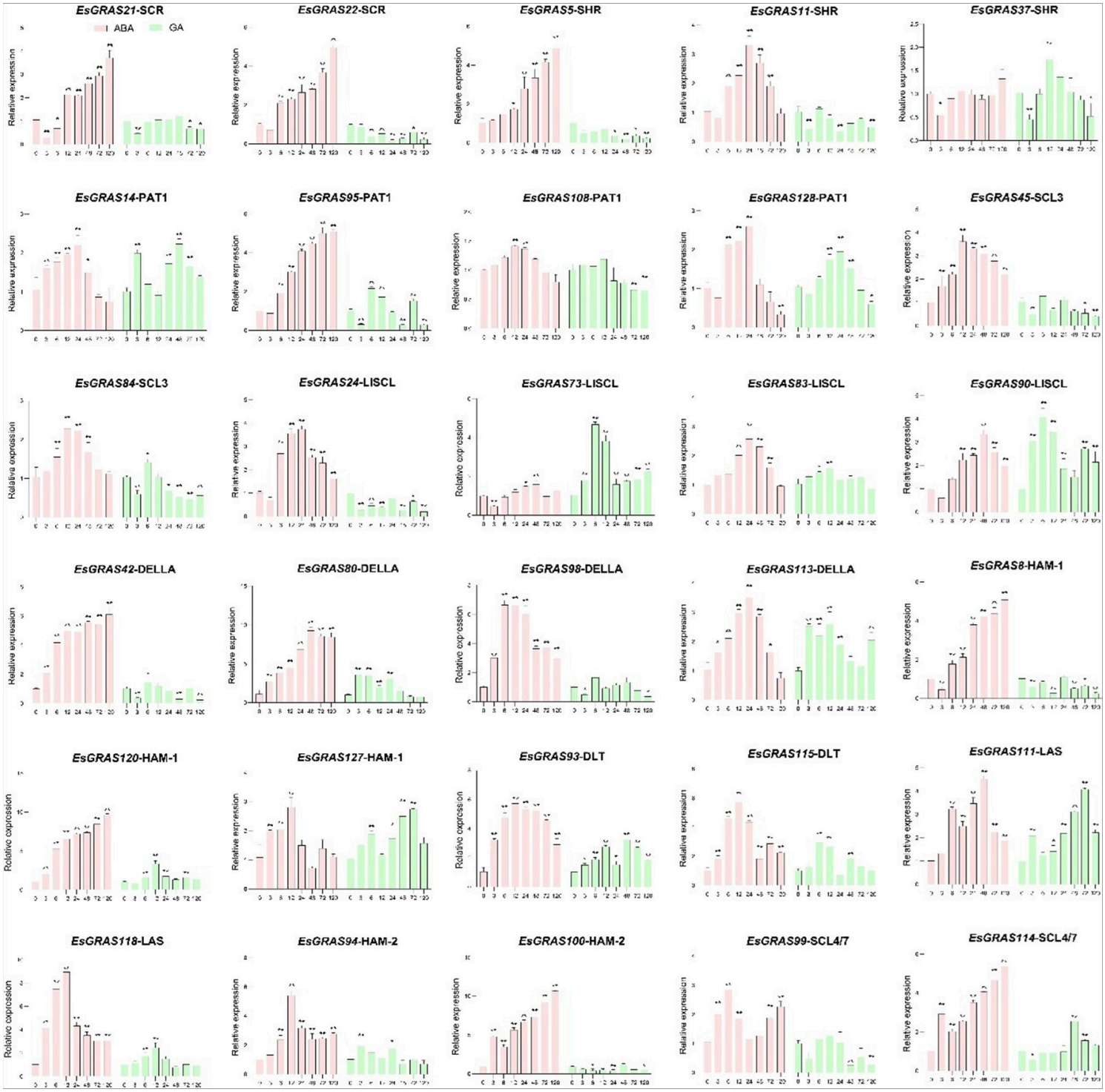

Figure 7

Expression of *GRAS* candidate genes under salt and drought stress treatments. The relative expression levels of these genes were quantified at specific time points: 0, 3, 6, 12, 24, 48, 72, and 100 hours for each treatment. The data presented are means ± standard deviation (SD) calculated from three independent biological replicates. To determine statistical significance, a one-way analysis of variance was conducted, and the results are indicated as follows: "*" denotes $P < 0.05$ and "**" denotes $P < 0.01$, n=6.

Supplementary Files

This is a list of supplementary files associated with this preprint. Click to download.

- Supplementarytable.xlsx
- SupplementaryFig.docx